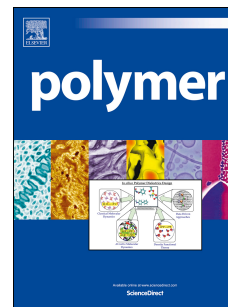


Accepted Manuscript

Self-assembled Polymeric Micelles Based on THP and THF Linkage for pH-Responsive Drug Delivery

Fangxia Zhu , Qinglai Yang , Yuan Zhuang , Yuanqing Zhang , Zhifeng Shao , Bing Gong , Yu-Mei Shen



PII: S0032-3861(14)00387-5

DOI: [10.1016/j.polymer.2014.05.010](https://doi.org/10.1016/j.polymer.2014.05.010)

Reference: JPOL 16963

To appear in: *Polymer*

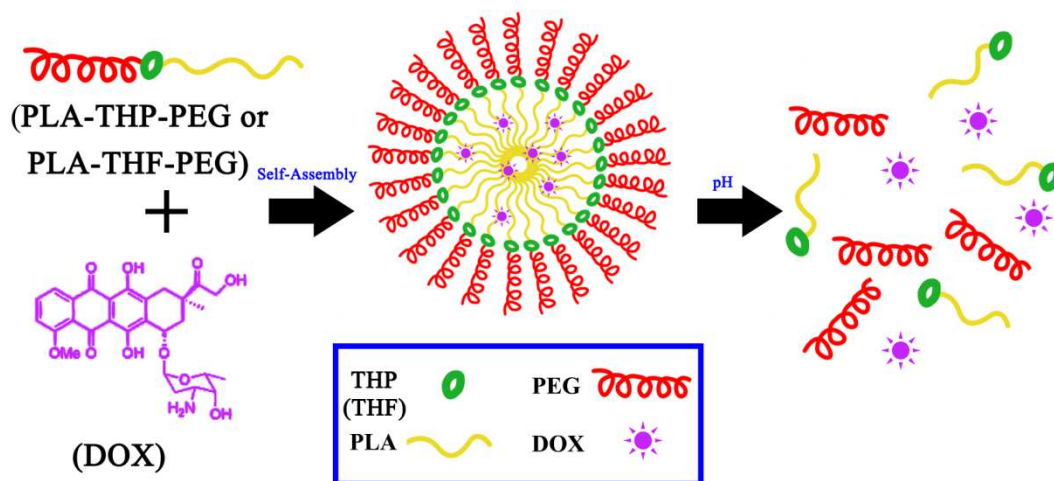
Received Date: 6 March 2014

Revised Date: 14 April 2014

Accepted Date: 6 May 2014

Please cite this article as: Zhu F, Yang Q, Zhuang Y, Zhang Y, Shao Z, Gong B, Shen Y-M, Self-assembled Polymeric Micelles Based on THP and THF Linkage for pH-Responsive Drug Delivery, *Polymer* (2014), doi: 10.1016/j.polymer.2014.05.010.

This is a PDF file of an unedited manuscript that has been accepted for publication. As a service to our customers we are providing this early version of the manuscript. The manuscript will undergo copyediting, typesetting, and review of the resulting proof before it is published in its final form. Please note that during the production process errors may be discovered which could affect the content, and all legal disclaimers that apply to the journal pertain.



ACCEPTED MANUSCRIPT

Self-assembled Polymeric Micelles Based on THP and THF

Linkage for pH-Responsive Drug Delivery

Fangxia Zhu[†], Qinglai Yang[†], Yuan Zhuang[†], Yuanqing Zhang[†], Zhifeng Shao[‡], Bing Gong^{||,§,*} and Yu-Mei Shen^{†,*}

[†]Shanghai Center for Systems Biomedicine, Key Laboratory of Systems Biomedicine and Bio-ID Center, Shanghai Jiao Tong University, Shanghai 200240, China

[‡]Shanghai Institute of Applied Physics, Chinese Academy of Sciences, Shanghai 201800, China

[‡]State Key Laboratory of Oncogenes and Bio-ID Center, School of Biomedical Engineering, Shanghai Jiao Tong University, Shanghai 200240, China

^{||}College of Chemistry, Beijing Normal University, Beijing 100875, China

[§]Department of Chemistry, University at Buffalo, State University of New York, Buffalo, NY 14260, United States

E-mail: yumeishen@sjtu.edu.cn; bgong@buffalo.edu

ABSTRACT: Developing smart nanocarriers for drug delivery system is advantageous for many kinds of successful biomedical therapy. In this study, we designed an amphiphilic block copolymers containing pH-responsive tetrahydropyran (THP) and tetrahydrofuran (THF) linkage. Their structures were confirmed by ^1H NMR and gel permeation chromatography (GPC). The release rate of encapsulated drugs depends upon the pH value and pH sensitive linkage in the backbone of copolymers. For PLA-THP-PEG micelles the cumulative release amount of doxorubicin (DOX) was 62% at pH 5.0, which is about four times higher than that at pH 7.4. Under the same conditions the release rate for PLA-THF-PEG micelles is a little faster than that of the PLA-THP-PEG micelles. Cellular uptake study demonstrates that DOX-loaded micelles can easily enter the cells and produce the desired pharmacological action and minimizing the side effect of free DOX. These findings indicate that THP and THF linked diblock copolymer micelles is a promising candidate for drug carrier.

KEYWORDS: Amphiphilic block copolymer; drug delivery; pH-responsive; doxorubicin

1. Introduction

A great challenge for hydrophobic anticancer drugs concerns limited availability of effective biocompatible delivery systems¹⁻¹². Poor water solubility is the major problem encountered with the anticancer drugs, so development of novel delivery systems attracted significant attention in the past decades. Block copolymer micelles with core-shell structures self-assembled from amphiphilic copolymers offer great potential

and promising approach to deliver hydrophobic drugs into tumor site¹³. The inner hydrophobic core and outer hydrophilic shell of the micelles can be used to load and protect hydrophobic drugs from inactivating under the biological environment. Recently stimuli-responsive polymeric micelles have emerged as vehicles for smart drug delivery based on the release of drugs can be readily modulated by exerting an appropriate stimulus such as temperature¹⁴⁻¹⁶, pH¹⁷⁻²⁰, glucose²¹⁻²², glutathione²³⁻²⁵, etc.²⁶⁻²⁸ Stimuli-responsive release of drugs may result in significantly enhanced therapeutic efficiency and minimal side effects²⁹⁻³⁰. Among available stimuli, pH responsiveness is particularly appealing due to pH values in malignant tissue from about 5.8 to 7.6³¹⁻³⁶. Therefore, pH-sensitive polymeric micelles which rapidly respond to the mild acidic pH trigger provide an opportunity for the achievement of programmable and controlled drug delivery. Tumoral pH variation has been considered as an ideal trigger for drug delivery based on the controlled release of anticancer drugs in tumor tissues and/or within tumor cells.

Up to now, a number of acid-cleavable linkers have been successfully adopted in the design and synthesis of pH-sensitive polymeric drug carriers³⁷⁻⁴⁴. While encouraging progress has been made in this field, new strategies that lead to further improvement on the responsive acuteness of the corresponding drug delivery systems are still in high demand.

Tetrahydropyran (THP) and tetrahydrofuran (THF) as protecting group widely used in organic synthesis have rarely been employed in constructing acid-responsive block copolymers⁴⁵⁻⁴⁶. In our current work, THP and THF will be used as an acid-responsive

unit in the formation of new pH-responsive block copolymers. We aim to obtain a novel and smart drug delivery system with THP and THF as pH-responsive linkage.

Herein we report the synthesis of amphiphilic block copolymers in which the hydrophilic poly(ethylene glycol) (PEG) and hydrophobic polylactic acid (PLA) are connected through THP or THF linkage and their self assembled micelles as potential acid sensitive nanocarriers. The micelles based on PLA-THP-PEG and PLA-THF-PEG copolymers were developed for intracellular delivery of doxorubicin (DOX), an effective anticancer drug. Their physical characteristics and pH-responsive properties of blank and drug-loaded micelles were observed by transmission electron microscopy (TEM), dynamic light scattering (DLS), in vitro drug release and confocal laser scanning microscopy (CLSM) measurements. Under physical conditions the micelles as potential drug delivery carriers remained stable up to 35 days, however under acidic conditions the pH sensitive linkage was cleaved and resulted in the release of encapsulated drugs. Therefore, the introduced THP and THF linkage in the backbone of copolymer drug carriers is the key structure which determines the release of encapsulated drugs.

2. Experimental section

2.1. Materials

All chemicals were purchased from Aldrich or Aladdin and were used as received unless otherwise mentioned. All reactions were monitored by thin-layer chromatography (precoated 0.25 mm silica gel plates from Aldrich). Flash column chromatography was carried out with silica gel 60 (mesh 200-400). *N, N*-dimethylformamide (DMF) was dried over calcium hydride and distilled under vacuum. Triethylamine (TEA) was refluxed

with phthalic anhydride, potassium hydroxide, and calcium hydride successively and then distilled before use. Monomethyl ether of PEG ($M_n = 1900, 5000$, determined by GPC) was purchased from Shanghai Yarebio Co. Ltd. PLA ($M_v = 1000, 3000, 5000$, determined by viscometry) was purchased from Jinan Daigang Biomaterial Co. Ltd. and used as received.

2.2. Methods

^1H and ^{13}C NMR analyses were recorded on a Bruker Avance III 400 MHz spectrometer with CDCl_3 as solvents. Tetramethylsilane (TMS) was used as the internal reference. Fourier transform infrared (FTIR) spectra were recorded by KBr sample holder method on a Perkin-Elmer Paragon 1000 instrument in the range of $4000\text{--}400\text{ cm}^{-1}$. Ultra Performance Liquid Chromatography with Tandem Level Four Pole Time of Flight Mass Spectrometry (UPLC-TOF-MS) was recorded on a Waters UMS Q-ToF Premier, UPLC conditions: Waters UPLC BEH C_{18} 1.0×100 mm column, 0.4 mL/min , methanol-water gradient elution; methanol 20% in 1 min followed by methanol 20% to 40% in 1 min, methanol 40% to 60% in 6 min, finally, methanol 60-95% in 2 min. The identity of each peak was confirmed by collecting the corresponding fraction that was then subjected to analysis by mass spectrometry. Number-average molecular weight (M_n) and polydispersity ($\text{PDI} = M_w/M_n$) were determined by GPC on an Agilent 1260 infinity GPC/SEC system ($10\text{ }\mu\text{m}$ PLgel 600×7.5 mm column, linear polystyrene calibration) equipped with a refractive index (RI) detector. The samples were estimated by GPC with THF as eluent, which contained 0.01 mol/L lithium bromide at a flow rate of 1 mL/min at $35\text{ }^\circ\text{C}$. Transmission Electron Microscopy (TEM) studies were performed with a JEOL JEM-100CX-II instrument at a voltage of 200 kV . Samples were prepared by

drop-casting micellar solution onto carbon-coated copper grids and then air-drying at room temperature overnight without staining before measurement. Dynamic Light Scattering (DLS) measurements were performed with a Malvern Zetasizer Nano S apparatus (Malvern Instruments Ltd.) equipped with a 4.0 mW He-Ne laser operating at = 633 nm. All samples (1 mg/mL) were measured in aqueous solution at room temperature (25 °C) and at a scattering angle of 173°.

2.3. Synthesis of PLA-THP-PEG copolymers

To an ice-cold solution of (3, 4-dihydro-2H-pyran-2-yl) methanol (925 mg, 8.1 mmol) in CH₂Cl₂ (40 mL), TEA (1.15 mL) was added, followed by 4-nitrobenzoyl chloride (2.02 g, 8.3 mmol). The reaction mixture was stirred at 0 °C for 1 h and then continued at room temperature for 4 h. The resulting mixture was washed with saturated sodium bicarbonate solution and extracted with ether. The combined organic extracts were washed with water and brine, dried over anhydrous magnesium sulfate (MgSO₄), filtered, followed by removing solvent. Purification was accomplished by column chromatography on silica gel by using dichloromethane/petroleum ether as eluent, which gave the desired intermediate **1** as a yellowish green liquid. Yield: 1.6 g, 75%. ¹H NMR (400 MHz, CDCl₃): δ 8.27-8.19 (m, 4H), 6.34 (d, *J* = 6.4 Hz, 1H), 4.75-4.65 (m, 1H), 4.50-4.38 (m, 2H), 4.20-4.12 (m, 1H), 2.20-2.08 (m, 1H), 2.05-1.95 (m, 1H), 1.95-1.85 (m, 1H), 1.80-1.70 (m, 1H); ¹³C NMR (100 MHz, CDCl₃): δ 164.6, 150.6, 143.3, 135.4, 131.0, 123.6, 100.7, 72.6, 67.5, 24.3, 19.2; IR (KBr): 3357, 3112, 3060, 2954, 2923, 2851, 1727, 1649, 1608, 1528, 1450, 1410, 1346, 1320, 1274, 1239, 1188, 1170, 1118, 1103, 1070, 1014, 968, 950, 888, 845, 788, 762, 718.

The intermediate **1** (1.689 g, 6.4 mmol) was dissolved in 45 mL of tetrahydrofuran (THF), to which a solution of NH_4Cl (1.368 g, 25.6 mmol) in water (30 mL) was added. Upon the mixture stirred at 70 °C for 30 min, Fe powder (1.428 g, 25.6 mmol) was added. The reaction mixture was stirred at 75 °C for another 50 h, cooled to room temperature, and then filtered through a celite pad. The filtrate was extracted with ethyl acetate. After being washed with saturated sodium bicarbonate solution and brine, and dried over anhydrous sodium sulfate, the organic extract was evaporated under reduced pressure. The residue was subjected to column chromatography (silica gel, petroleum ether/ethyl acetate) to give the desired intermediate **2** as a cream-coloured solid. Yield: 1.16 g, 77.7%. ^1H NMR (400 MHz, CDCl_3): δ 7.86 (d, J = 8.8 Hz, 2H), 6.61 (d, J = 8.8 Hz, 2H), 6.39 (d, J = 6.0 Hz, 1H), 4.75-4.65 (m, 1H), 4.38-4.34 (m, 2H), 4.18-4.11 (m, 1H), 2.18-2.07 (m, 1H), 2.06-1.96 (m, 1H), 1.95-1.87 (m, 1H), 1.82-1.71 (m, 1H); ^{13}C NMR (100 MHz, CDCl_3): δ 166.6, 151.2, 143.5, 131.9, 119.4, 113.8, 100.6, 73.1, 66.1, 24.5, 19.3; IR (KBr): 3466, 3368, 3231, 3060, 2951, 2923, 2850, 1694, 1648, 1626, 1602, 1518, 1439, 1310, 1273, 1239, 1171, 1112, 1067, 1013, 973, 843, 770, 729, 699.

Under nitrogen atmosphere, PLA (1 mmol) and 2-(7-aza-1H-benzotriazole-1-yl)-1,1,3,3-tetramethyluronium hexafluorophosphate (HATU) (2 mmol) were dissolved in 30 mL DMF, then N, N-diisopropylethylamine (DIPEA) (4 mmol) was added and the reaction was stirred at 0 °C for 0.5 h. After adding the intermediate **2** (2 mmol, dissolved in 4 mL DMF) the reaction mixture was stirred at 30 °C for an additional 45 h. The resulting mixture was poured into a few drops of concentrated hydrochloric acid and extracted with CH_2Cl_2 . The combined organic extracts were washed with water and brine, dried over anhydrous magnesium sulfate, filtered, and the filtrate was evaporated.

Purification was accomplished by chromatography to give the desired intermediate **3** as yellow semi-solid product.

3a, yield: 81%. ^1H NMR (400 MHz, CD_3OD): δ 8.04-7.96 (m, 3H), 7.63-7.55 (m, 2H), 6.38 (d, $J = 6.4$ Hz, 1H), 5.20-5.05 (m, 53H), 4.72-4.66 (m, 1H), 4.40-4.35 (m, 2H), 4.20-4.10 (m, 12H), 2.85-2.61 (m, 13H), 2.20-2.10 (m, 1H), 2.09-1.99 (m, 2H), 1.98-1.85 (m, 1H), 1.61-1.38 (m, 168H); ^{13}C NMR (100 MHz, CDCl_3): δ 172.4, 170.4, 169.6, 169.4, 166.1, 143.3, 142.5, 130.9, 125.1, 118.9, 100.6, 72.8, 69.3, 66.5, 31.9, 29.1, 24.3, 19.2, 16.6; IR (KBr): 3371, 2993, 2944, 1755, 1649, 1598, 1530, 1453, 1409, 1383, 1364, 1308, 1273, 1189, 1130, 1094, 1051, 860, 770, 741, 698, 665.

3b, yield: 68%. ^1H NMR (400 MHz, CD_3OD): δ 8.29 (s, 1H), 8.02-7.94 (m, 2H), 7.63-7.55 (m, 2H), 6.36 (d, $J = 6.0$ Hz, 1H), 5.20-5.04 (m, 15H), 4.72-4.66 (m, 1H), 4.39-4.35 (m, 2H), 4.20-4.12 (m, 5H), 2.84-2.76 (m, 2H), 2.76-2.60 (m, 3H), 2.20-2.06 (m, 1H), 1.98-1.94 (m, 2H), 1.80-1.70 (m, 1H), 1.62-1.42 (m, 47H); ^{13}C NMR (100 MHz, CDCl_3): δ 174.5, 171.2, 169.7, 169.2, 165.4, 143.1, 130.5, 124.5, 118.4, 100.2, 72.5, 69.0, 66.3, 38.3, 36.2, 31.1, 24.7, 20.1, 16.3; IR (KBr): 3502, 2994, 2944, 1756, 1648, 1599, 1530, 1455, 1409, 1383, 1364, 1305, 1270, 1186, 1131, 1093, 1046, 955, 868, 756, 701.

3c, yield: 64%. ^1H NMR (400 MHz, CDCl_3): δ 8.05-7.98 (m, 2H), 7.82-7.56 (m, 2H), 6.39 (d, $J = 6.4$ Hz, 1H), 5.26-5.08 (m, 68H), 4.77-4.68 (m, 1H), 4.42-4.38 (m, 2H), 4.20-4.16 (m, 2H), 2.86-2.78 (m, 7H), 2.78-2.66 (m, 2H), 2.20-2.10 (m, 1H), 2.08-2.01 (m, 12H), 2.00-1.90 (m, 1H), 1.68-1.46 (m, 223H); ^{13}C NMR (100 MHz, CDCl_3): δ 174.8, 171.0, 169.4, 169.3, 169.1, 143.4, 130.8, 126.8, 125.6, 119.3, 118.7, 100.5, 72.7,

69.1, 66.5, 38.5, 29.6, 24.3, 20.9, 16.7; IR (KBr): 3502, 2995, 2945, 1755, 1648, 1599, 1530, 1455, 1382, 1365, 1319, 1270, 1188, 1131, 1092, 1051, 956, 865, 739, 701.

PEG (0.5 mmol) was dissolved in 1, 2-dichloroethane (1, 2-DCE) (90 mL) and pyridinium p-toluenesulfonate (PPTS) solution (0.5 mmol). After stirring at room temperature for 15 min, the intermediate **3** (0.5 mmol) was added. The reaction was refluxed at 95 °C for 24 h. Then the solvent was evaporated and purified by chromatography to give the desired terminal product block copolymer **4** as solid. An inseparable mixture of trans/cis diastereomers was observed for the terminal product **4** in some cases.

4a (PLA₁₀₀₀-THP-PEG₁₉₀₀). Yield: 50.9%. ¹H NMR (400 MHz, CDCl₃) δ 8.00-7.94 (m, 2H), 7.78-7.58 (m, 2H), 5.24-5.08 (m, 14H), 4.88 (s, 1H), 4.40-4.26 (m, 2H), 4.26-4.22 (m, 2H), 3.90-3.42 (m, 206H), 3.36 (s, 3H), 2.84-2.75 (m, 2H), 2.75-2.60 (m, 2H), 1.96-1.70 (m, 6H), 1.70-1.40 (m, 49H); ¹³C NMR (100 MHz, CDCl₃): δ 172.0, 170.1, 169.2, 169.1, 165.8, 143.2, 130.4, 125.5, 119.2, 118.5, 100.3, 97.0, 77.4, 72.3, 70.3, 68.8, 67.6, 58.8, 31.7, 29.4, 24.1, 18.9, 16.0; IR (KBr): 3502, 2868, 1755, 1713, 1599, 1536, 1454, 1410, 1383, 1350, 1272, 1255, 1186, 1103, 1040, 991, 952, 860, 771, 700, 577.

4b (PLA₃₀₀₀-THP-PEG₁₉₀₀). Yield: 18.6%. ¹H NMR (400 MHz, CDCl₃) δ 8.02-7.92 (m, 2H), 7.68-7.58 (m, 2H), 5.22-5.08 (m, 20H), 4.87 (s, 1H), 4.42-4.20 (m, 2H), 4.20-4.10 (m, 6H), 3.85-3.41 (m, 191H), 3.35 (s, 3H), 2.90-2.77 (m, 2H), 2.77-2.60 (m, 6H), 1.96-1.60 (m, 10H), 1.60-1.46 (m, 63H); ¹³C NMR (100 MHz, CDCl₃): δ 174.8, 172.1, 170.1, 169.4, 165.8, 142.9, 130.5, 124.6, 118.5, 102.2, 97.1, 71.7, 70.4, 69.1, 68.3,

64.6, 58.8, 31.7, 29.1, 24.8, 20.3, 16.9; IR (KBr): 3501, 2921, 2871, 1755, 1716, 1598, 1534, 1455, 1409, 1384, 1354, 1271, 1257, 1212, 1185, 1129, 1095, 1043, 994, 952, 862, 771, 756, 700.

4c (PLA₃₀₀₀-THP-PEG₅₀₀₀). Yield: 12.7%. ¹H NMR (400 MHz, CDCl₃) δ 7.98-7.92 (m, 2H), 7.66-7.60 (m, 2H), 5.21-5.04 (m, 20H), 4.86 (s, 1H), 4.37-4.20 (m, 2H), 4.20-4.14 (m, 5H), 3.81-3.41 (m, 501H), 3.35 (s, 3H), 2.88-2.73 (m, 3H), 2.73-2.62 (m, 4H), 2.02-1.66 (m, 6H), 1.60-1.46 (m, 64H); ¹³C NMR (100 MHz, CDCl₃): δ 174.6, 171.9, 171.2, 169.7, 169.2, 165.7, 142.8, 130.3, 124.4, 118.4, 102.1, 96.9, 77.4, 71.6, 70.2, 68.7, 64.4, 58.7, 31.1, 29.3, 24.7, 20.2, 16.3; IR (KBr): 3502, 2869, 1758, 1715, 1647, 1560, 1534, 1455, 1409, 1383, 1350, 1298, 1255, 1184, 1100, 1042, 994, 950, 861, 771, 701.

4d (PLA₅₀₀₀-THP-PEG₅₀₀₀). Yield: 12.7%. ¹H NMR (400 MHz, CDCl₃) δ 8.02-7.96 (m, 2H), 7.78-7.60 (m, 2H), 5.25-5.10 (m, 76H), 4.89 (s, 1H), 4.41-4.30 (m, 2H), 4.28-4.24 (m, 1H), 3.84-3.42 (m, 427H), 3.36 (s, 3H), 2.88-2.75 (m, 2H), 2.75-2.60 (m, 2H), 1.94-1.66 (m, 6H), 1.64-1.42 (m, 243H); IR (KBr): 3504, 2902, 2863, 1755, 1715, 1705, 1454, 1384, 1362, 1269, 1186, 1128, 1092, 1046, 952, 862, 798, 739, 706.

Similarly the diblock copolymers PLA-THF-PEG **18** were synthesized and characterized accordingly, the detailed procedure was in supporting information.

2.4. Preparation of blank and DOX-loaded micelles

In brief, one of the copolymers PLA-THP-PEG (**4a**, **4b**, **4c**, **4d**) and PLA-THF-PEG (**18a**, **18b**, **18c**) (10 mg) was dissolved in 1 mL of DMF and stirred at room temperature. The solution was then added slowly to 8 mL of deionized water and stirred for another 1

hr. Subsequently, the solution was dialyzed against deionized water for 24 hrs using dialysis tubing having molecular weight cut off (MWCO) of 2000, with the deionized water being changed every 5 hrs. The appearance of turbidity in the aqueous solution indicated the formation of aggregations. DOX-loaded micelles were prepared as above. Besides, adding 1 mg of DOX·HCl and 1.5 equivalents of triethylamine to the solution. In order to confirm that no more free DOX could be removed by dialysis, the change of the fluorescent emission intensity of dialysate with time was monitored. To determine the drug loading content (DLC) and drug loading efficiency (DLE), the DOX-loaded micelle solution was lyophilized and dissolved in DMSO. The fluorescence excitation spectra at 485 nm was measured to determine the DOX concentration based on the standard curve of the fluorescence excitation spectra of DOX in DMSO solution. DLC and DLE were calculated according to the following formula:

$$\text{DLC (wt \%)} = (\text{weight of loaded drug} / \text{weight of polymer}) \times 100\%$$

$$\text{DLE (\%)} = (\text{weight of loaded drug} / \text{weight of drug in feed}) \times 100\%$$

2.5. CMC measurement

The change of fluorescence emission of pyrene was plotted against the corresponding concentration of the block copolymer, leading to the determination of critical micelle concentration (CMC). Pyrene was dissolved in acetone and added to 5 mL volumetric flasks to the concentration of 6.4×10^{-3} mM in the final solutions. Acetone was then evaporated and replaced with aqueous polymeric micelle solution with concentrations ranging from 5.0×10^{-5} to 5.0×10^{-1} mg/mL. Samples were stirred at room temperature for 24 hrs. The emission wavelength and excitation bandwidth were set at

334 and 5 nm respectively. The intensity ratio of peaks at 373 nm to those at 384 nm was plotted against the logarithm of copolymer concentration to measure CMC.

2.6. Evaluation of Drug Release

A solution (2.5 mL) of DOX-loaded PLA-THP-PEG and PLA-THF-PEG micelles, prepared as described above, was transferred into a membrane bag with a MWCO of 2000. The membrane bag was immersed in 200 mL of phosphate buffer (pH 7.4) or pH 5.0 solutions in a shaking water bath at 37 °C to acquire sink conditions. At predetermined time intervals, 2.5 mL of the external buffer was withdrawn and replenished with an equal volume of fresh media for analysis. Drug release study was performed for 100 hrs. The amount of released DOX was analyzed with fluorescence measurement (BioTek Synergy 2, excitation wavelength at 485 nm, emission wavelength at 490 nm). All DOX-release experiments were performed in triplicate, and the results were the average data with standard deviations.

2.7. Confocal laser scanning microscope (CLSM) studies

CLSM was utilized to visualize the cellular internalization and investigate the intracellular distribution of DOX-loaded micelles and free DOX. For the CLSM study, HeLa cells were seeded in 6-well plates at 2×10^6 cells per well in 1 mL complete DMEM and cultured for 24 hrs, followed by removing culture medium and adding DMEM solution of free DOX and DOX-loaded micelles at finally the DOX concentration of 9 µg/mL, respectively. The cells were incubated at 37 °C for the predetermined interval 60 min and then washed with PBS and fixed with 4% paraformaldehyde at room temperature for 30 min before the cell nucleus were stained by DAPI

(4',6-diamidino-2-phenylindole) (excitation/emission: 486 nm/596 nm) for 10 min. Thereafter, the slides were rinsed with PBS for three times and cover slips were placed onto glass microscope slides. Finally the slides were installed and observed with CLSM.

2.8. In vitro cell assay

The cytotoxicity of DOX-loaded PLA-THP-PEG, PLA-THF-PEG micelles and free DOX against HeLa cancer cells was evaluated by 3-(4, 5-dimethylthiazol-2-yl)-2, 5-diphenyl tetrazolium bromide (MTT) assay. The cells were seeded in 96-well plates with a density of 1×10^4 cell per well and were cultured in 200 μ L DMEM at 37 °C under atmosphere containing 5% CO₂ for 24 hrs to allow cell attachment. Then, the medium was replaced with 200 μ L fresh medium containing the indicated concentration of DOX-loaded PLA-THP-PEG, PLA-THF-PEG micelles and free DOX. After incubation for 48 h, the medium was aspirated and replaced by 100 mL of fresh medium containing 20 μ L 5 mg mL⁻¹ of MTT. After 4 hrs, the medium was replaced by 200 μ L DMSO. Afterward, the absorbance at a wavelength of 490 nm of each well was measured using a microplate reader. The relative cell viability (in percentage) was determined by the following equation:

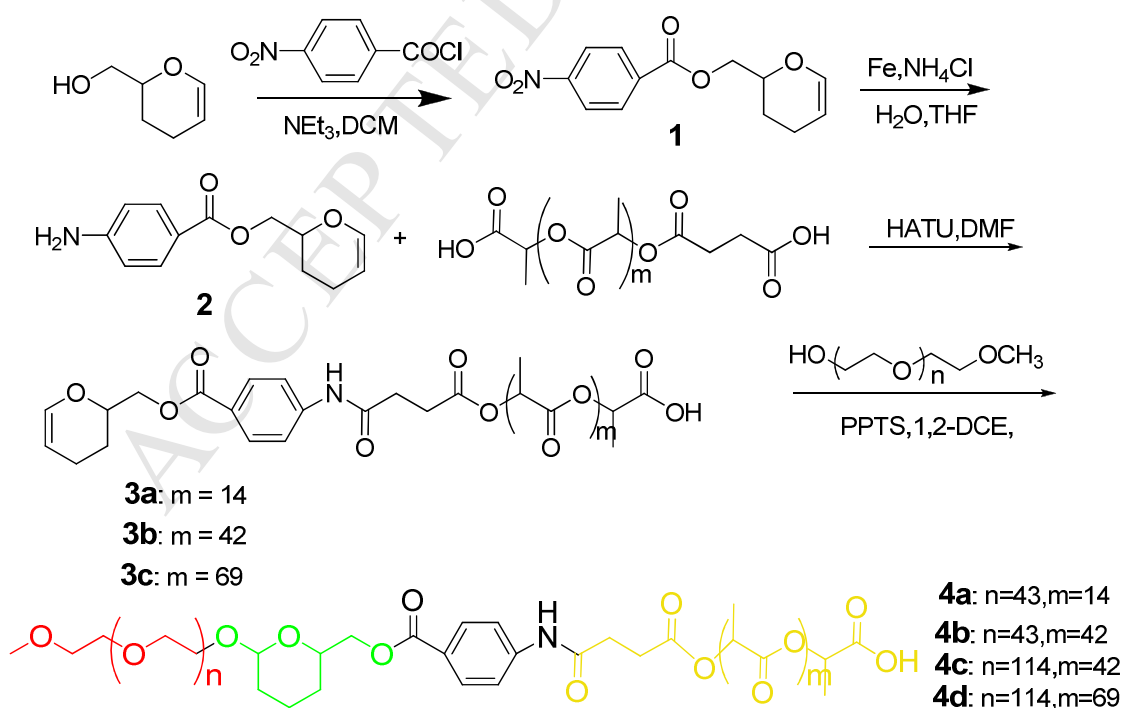
$$\text{Cell viability (\%)} = (I_{\text{sample}} - I_{\text{blank}}) / (I_{\text{control}} - I_{\text{blank}})$$

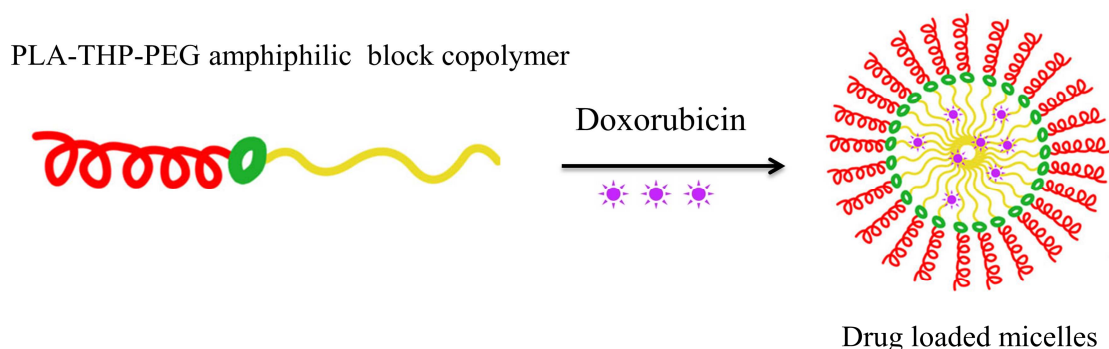
Where I_{sample} , I_{control} , and I_{blank} represents the absorbance intensity at 490 nm determined for cells treated with sample containing different amounts of DOX, for control cells (nontreated), for blank well without cells, respectively.

3. Results and discussion

3.1. Synthesis and Characterization

To design block copolymers containing THP or THF linkages in the backbone, the intermediate **3** with the dihydropyran (DHP) terminals was prepared by condensation of carboxyl group in PLA with the amine in modified DHP moiety. The synthetic route of PLA-THP-PEG was shown in Scheme 1. First, the carboxyl group of macromolecular PLA was reacted with the amine terminals of the DHP with the feeding molar ratio of 1:2, affording the intermediate product **3**. The molecular weight of DHP modified PLA was determined directly by the starting material PLA. Subsequently, the intermediate **3** was further coupled to different molecular weight of PEG by DHP group reacted with hydroxyl group of PEG, resulted in the formation of terminal product PLA-THP-PEG (**4**) as diblock copolymer.





Scheme 1 Synthesis and self-assembly of diblock copolymer PLA-THP-PEG

For diblock copolymers PLA-THF-PEG **18** (see supplementary material Scheme S1), the synthetic route has a little difference with that of copolymers PLA-THP-PEG **4**. First, the hydroxyl group of PEG was condensed with hydroxyl group in modified tetrahydrofuran (THF), affording THF modified PEG **16** with nitro functional ends. Followed by reduction of the nitro group to amine catalyzed by Pd/C to give THF-modified PEG **17**. Accordingly, the amine group in the intermediate **17** was further reacted with carboxyl group of PLA to afford the terminal product diblock copolymers PLA-THF-PEG **18**.

Figure 1A and 1B provides the ^1H NMR spectra of the intermediate **3c** and the terminal product diblock copolymer PLA-THP-PEG **4d**. The signal around 6.39 and 4.72 ppm in Figure 1A corresponds to the characteristics of DHP. After the following coupled reaction with PEG, the DHP signal disappeared as shown in Figure 1B. Meanwhile, the signal at 4.87 ppm suggested the successful coupling of the intermediate **3c** with the hydroxyl terminal of PEG monomethyl ether to give the terminal product **4d**. Similarly from the ^1H NMR spectra of the intermediate **17b** (Figure 1C) and the terminal product diblock copolymer PEG-THF-PLA **18c** (Figure 1D), the signal of 5.33 corresponds to the THF characteristics, the signals of 5.13, 2.68 and 1.50-1.60 ppm corresponds to PLA,

and the signals of 3.35 and 3.45-3.75 ppm corresponds to PEG segment in Figure 1D. Therefore, ^1H NMR spectra in Figure 1 elucidate the successful synthesis of the intermediates and the terminal products PLA-THP-PEG **4d** and PLA-THF-PEG **18c**.

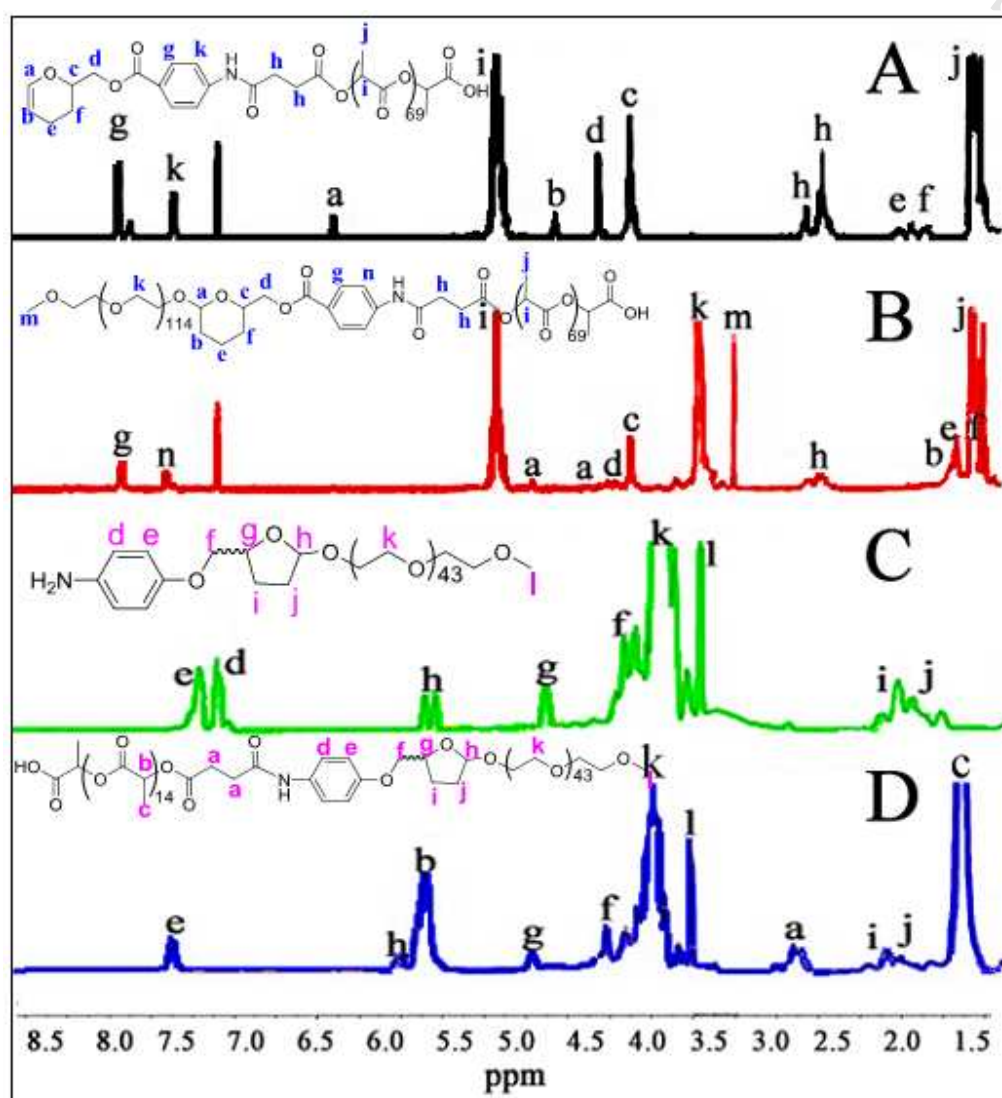


Figure 1 ^1H NMR spectra of (A) modified PLA **3c** ($m = 69$) (B) the terminal product **4d** ($m = 69$, $n = 114$) (C) intermediate **17b** ($n = 114$) (D) the terminal product **18c** ($m = 69$, $n = 114$) (400 MHz, CDCl_3 , 298 K).

The proposed structure of the block copolymers PEG-THP-PLA and PEG-THF-PLA was further confirmed by the gel permeation chromatography (GPC) traces (Figure S19).

Table 1 lists the number-average molecular weights and polydispersity index (PDI) of PEG, the intermediate **3**, the terminal product **4**, PLA, modified PEG **17** and the terminal product diblock copolymers **18**. All the GPC traces of PLA-THP-PEG and PLA-THF-PEG showed monomodal symmetric distribution. The GPC profile of the block copolymers PLA-THP-PEG and PLA-THF-PEG compared with their precursor modified PLA or modified PEG affords an evident shift toward higher molecular weight, suggesting successful coupling between PEG and PLA via THP or THF linkage. For typical terminal product **4d** the number-average molecular weight is 10×10^3 , with a PDI value of 1.08. The other copolymers with different molecular weight gave similar results. Moreover, the amphiphilic block copolymers display a good solubility in common organic solvent, like THF, DMF, and DMSO. Besides, this polymeric amphiphile can make itself spontaneously aggregate in aqueous media due to the common amphiphilic nature, which is beneficial for further biomedical applications.

Table 1 GPC Data of PEG, the intermediate **3**, terminal product **4**, PLA, intermediate **17** and terminal product **18**^a

Polymer	$M_n(\times 10^3)$	$M_w(\times 10^3)$	PDI
PEG ₁₉₀₀	2.1	2.2	1.04
PEG ₅₀₀₀	5.1	5.4	1.07
3a	1.9	3.2	1.65
3b	3.4	4.2	1.23
3c	6.1	8.3	1.35
4a	3.4	3.9	1.13
4b	4.3	4.8	1.12
4c	7.6	8.2	1.08
4d	10	11	1.08
PLA ₁₀₀₀	1.0	1.7	1.82
PLA ₃₀₀₀	1.2	3.4	2.80
PLA ₅₀₀₀	3.7	6.0	1.62
17a	2.0	2.0	1.03

17b	4.5	5.0	1.10
18a	2.8	3.1	1.12
18b	7.8	8.4	1.08
18c	11	13	1.23

^aEstimated by GPC (THF, 1 mL/min) using polystyrene standards.

3.2. Self-Assembly of Block Copolymers

Considering that the critical micelle concentration (CMC) is one of the most important parameters for micelles, the CMC value of PLA-THP-PEG and PLA-THF-PEG in water was investigated. The determination of CMC was further verified the successful formation of PLA-THP-PEG and PLA-THF-PEG micelles in aqueous media. CMC value was determined by using pyrene as a fluorescent probe. In the process of aggregation, the absorbance of DHP is close to zero when the concentration is below the CMC value, whereas absorbance intensity of DHP is enhanced exponentially with the growing concentration when the hydrophobic probe is encapsulated into the micelles. Therefore a graph with the intensity ratio I_{373}/I_{384} of two linear segments having two different slopes was obtained. The intersection point of the two segments gave the CMC value (Figure S20). As shown in Table 2, the CMC of each micelles⁴⁷ being in the range of 10^{-6} M, indicating the high stability characteristics of polymeric micelles⁴⁸. Further the CMC value was decreased when the molecular weight of copolymers was increased (Table 2). These results confirmed that the molecular weight of the copolymers are larger, the resultant micelles will be more stable⁴⁹.

To further study the properties of the polymeric micelles, both DLS and TEM measurements were performed. Diameter and PDI of PLA-THP-PEG and PLA-THF-PEG micelles were characterized by DLS. The results from DLS showed that

all of the micelles exhibited unimodal size distribution, with mean diameters ranging from 19 nm to 53 nm (Table 2). As shown in Table 2, the average diameter of the micelles increases with the length of the hydrophobic PLA block, while the size of the PEG block has little effect on the diameter of the micelles. The longer hydrophobic PLA block leads to enhanced hydrophobicity and more convenient self-assembly process driven by hydrophobic interaction. A typical TEM image of the blank micelles formed from copolymer **4d** and **18c** was shown in Figure 2A and Figure 2B respectively which appear approximately spherical. Both of the size of the micelles **4d** (Figure 2C) and **18c** (Figure 2D) determined by DLS was in accordance with the data from TEM.

Table 2 Properties of the PLA-THP-PEG **4** and PLA-THF-PEG **18** micelles

Copolymer	Diameter ^a (nm)	PDI ^a	CMC ^b (10 ⁻⁶ M)
4a	28	0.274	10.5
4b	31	0.245	6.2
4c	41	0.201	2.8
4d	40	0.124	1.7
18a	30	0.156	12.5
18b	32	0.157	2.6
18c	53	0.200	1.6

^aDiameter and polydispersity index (PDI) of micelles were determined by dynamic light scattering (DLS); ^bCritical micelle concentration (CMC) was determined by UV/vis spectrometer.

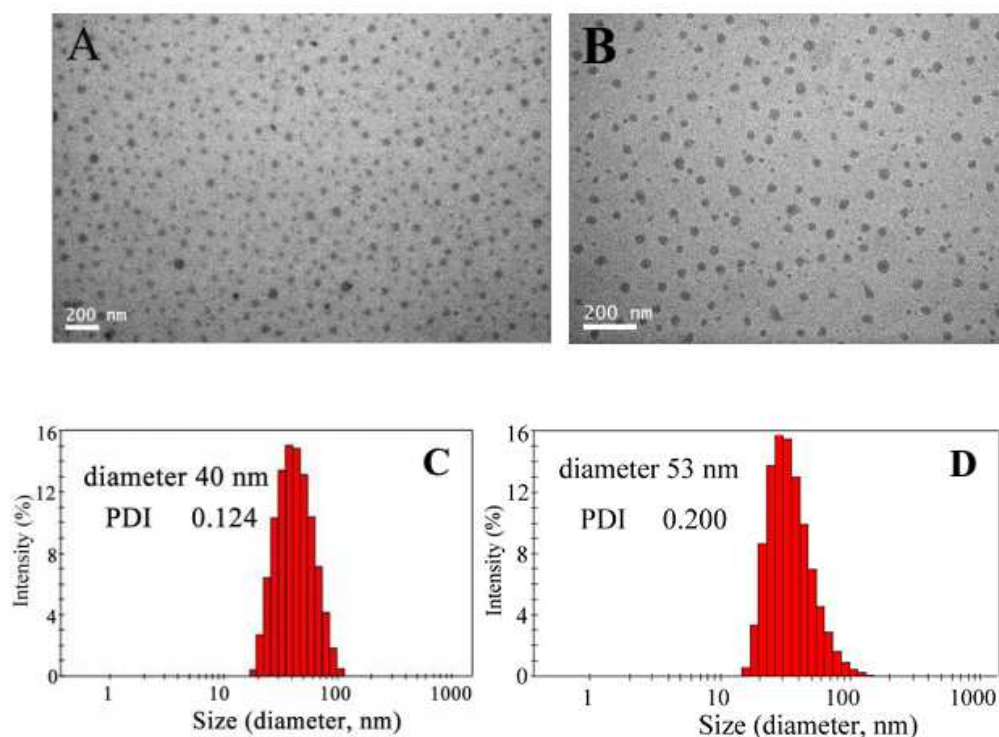
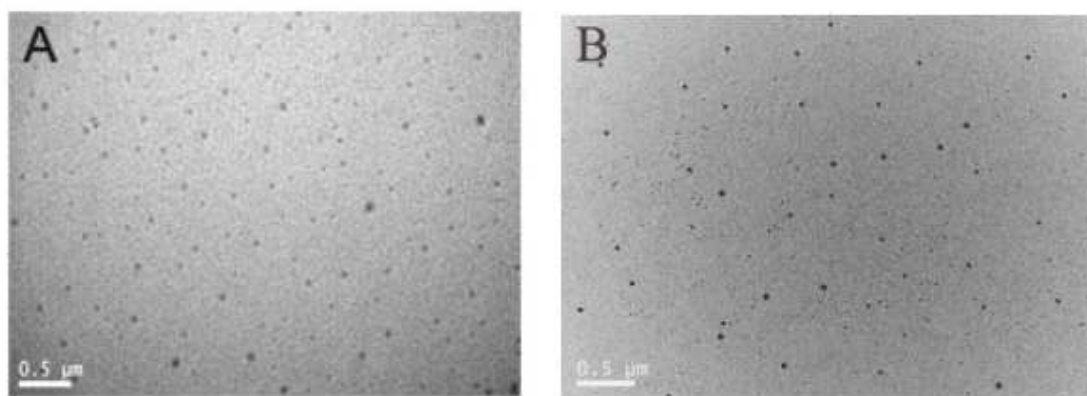


Figure 2 TEM image of (A) **4d** and (B) **18c** micelles; DLS measurement of the hydrodynamic diameter of micelles (C) **4d** and (D) **18c** in aqueous solution.

3.3. Size and morphology of DOX-loaded micelles 4 and 18

Doxorubicin (DOX) is one of the most widely used antitumor drugs, which acts by inhibiting the synthesis of nucleic acids in tumor cells. The polymeric micelles described above had a size distribution in the range of 19 to 53 nm, which affords the polymeric micelles passive targeting function to tumor tissues via the enhanced permeability and retention (EPR) effect⁵⁰. Furthermore, the micelles described here were characterized with core-shell architecture. Thus, hydrophobic drugs could be entrapped into the core, and the hydrophilic shell could effectively protect the core against the external biological media, inhibit nonspecific protein absorption, and increase the plasma clearance of half-life. In this paper, DOX as a model drug was encapsulated into the micelles, and the

drug loading content of micelles **4d** and **18c** were 13.0% and 14.3%, respectively (Figure S27). The morphology of the DOX-loaded micelles in aqueous solution was studied by TEM technique. As shown in Figure 3A and 3B, spherical micelles with an average diameter of about 80 nm were observed for both **4d** and **18c**. To further confirm the TEM observation, DLS measurements were performed to analyze the hydrodynamic diameter of the DOX-loaded micelles. Figure 3C and 3D showed the average size of the DOX-loaded micelles **4d** and **18c** were 131 nm and 130 nm with a PDI value of 0.155 and 0.148 respectively, which is larger than that of blank micelles while still kept narrow distribution in aqueous media. The size of the micelle is decided by the hydrophobic core and DOX as hydrophobic drug which easily associated with the hydrophobic block of the micelle. Therefore, the size of micelle increased upon DOX was loaded⁵¹. Moreover, the size of micelles observed with DLS was also larger than that of TEM. The smaller size measured by TEM as compared to DLS was most probably due to shrinkage of the PEG shell upon drying.



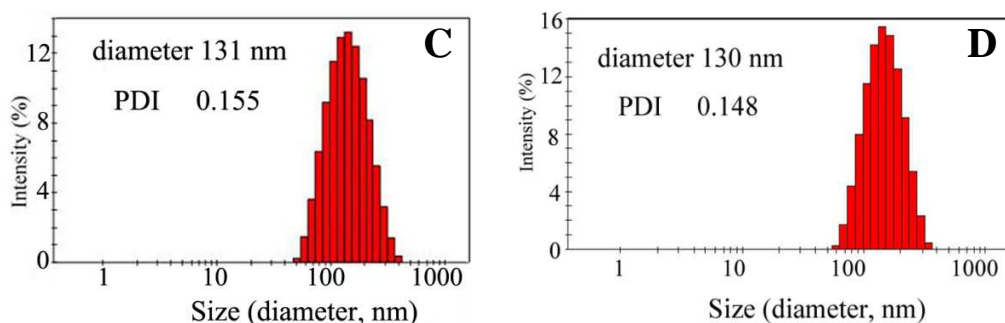


Figure 3 TEM image of DOX-loaded micelle (A) **4d** and (B) **18c**; DLS measurement of the hydrodynamic diameter of DOX-loaded micelle (C) **4d** and (D) **18c** in aqueous solution.

3.4. Stability and pH Responsiveness of Blank and DOX-Loaded Micelles 4 and 18

The stability of blank micelles **4** and **18** was studied at room temperature using DLS (Figure S24 and S25). As shown in Figure 4, the micelles **4d** and **18c** remained stable up to 35 days (Figure 4A) and 32 days (Figure 4C) at room temperature in the absence of acid, respectively. Furthermore, the DOX-loaded micelle **4d** was examined under various acidic conditions as shown in Figure 4B which remained stable for up to 4 hrs at 37 °C and pH 6.8, its average diameter increases from 100 nm to 1000 nm after 13 hrs. Similarly as shown in Figure 4D, the DOX-loaded micelle **18c** began to change at 6 hrs and the size of micelles increases from 62 nm to 258 nm after 10 hrs. The driving force for the change of micelle size at low pH value is attributed to the cleavage of THP or THF linkage, which leads to the shedding of hydrophilic PEG shell from the micelles and the aggregation of hydrophobic PLA core⁵². Under acid conditions the micelles was degraded and the hydrophobic PLA core aggregated to become larger. In contrast, no obvious change in micelle size was observed after 35 days and 32 days at pH = 7.4 for blank micelle **4d** (Figure 4A) and **18c** (Figure 4B), respectively. From these results it can be concluded that the prepared micelles is highly stable and the release behavior is pH

dependent. That is, significantly faster drug release at mildly acidic pH 6.8 compared to that of physiological pH. These pH-responsive biodegradable micelles are promising as smart nanovehicles for delivery of anticancer drugs.

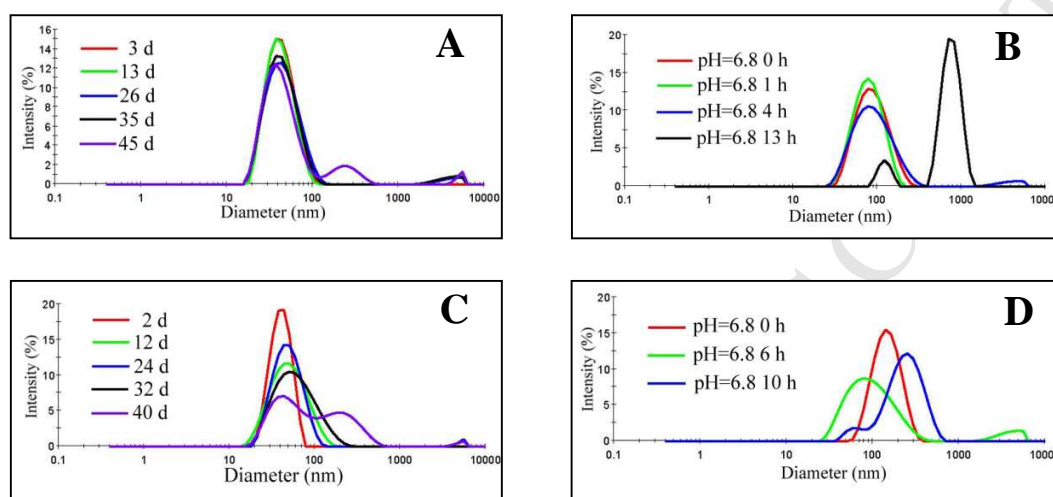


Figure 4 DLS plots of size change of micelles (A) blank **4d** (25 °C, pH 7.4); (B) DOX-loaded **4d** (37 °C, pH 6.8); (C) blank **18c** (25 °C, pH 7.4); (D) DOX-loaded **18c** (37 °C, pH 6.8).

3.5. In Vitro Drug Release

As an initial test to verify the utility of prepared DOX-loaded PLA-THP-PEG and PLA-THF-PEG micelles for drug release, the *in vitro* drug release profiles were monitored at pH 7.4 and 5.0 by fluorescence spectrophotometry. As shown in Figure 5, DOX release under physiological conditions (pH 7.4) was significantly lower than that under acidic conditions (pH 5.0) for both DOX-loaded PLA-THP-PEG and PLA-THF-PEG micelles. The accumulated drug release was 62% for PLA-THP-PEG micelles and 69% for PLA-THF-PEG micelles at pH 5.0 within 100 hrs, respectively. In contrast, the release was 16% for PLA-THP-PEG micelles and 20% for PLA-THF-PEG

micelles at pH 7.4, respectively. The drug release from micelles PLA-THF-PEG is a little faster than that from PLA-THP-PEG micelle under the same pH conditions due to the linkage THF is more acid sensitive than THP. In contrast, the drug release profile of DOX-loaded PLA-PEG micelles without pH-sensitive linkage (PLA-PEG) was also carried out under the same conditions. Both of the release amounts were less than 7% at pH 7.4 and pH 5.0, indicating the significant role of THP and THF linker in pH responsiveness.

Although the mechanism of drug release from polymeric matrices is very complex and is still not completely understood, it can be simplistically classified as either pure diffusion, erosion controlled release or a combination of the two mechanisms⁵³. In this study, we supposed that the release of DOX from PLA-THP-PEG and PLA-THF-PEG copolymer micelles under acidic conditions may be determined by the cleavage of pH-sensitive linkages and eventually lead to the micelle size increases as the copolymers degrade at low pH.

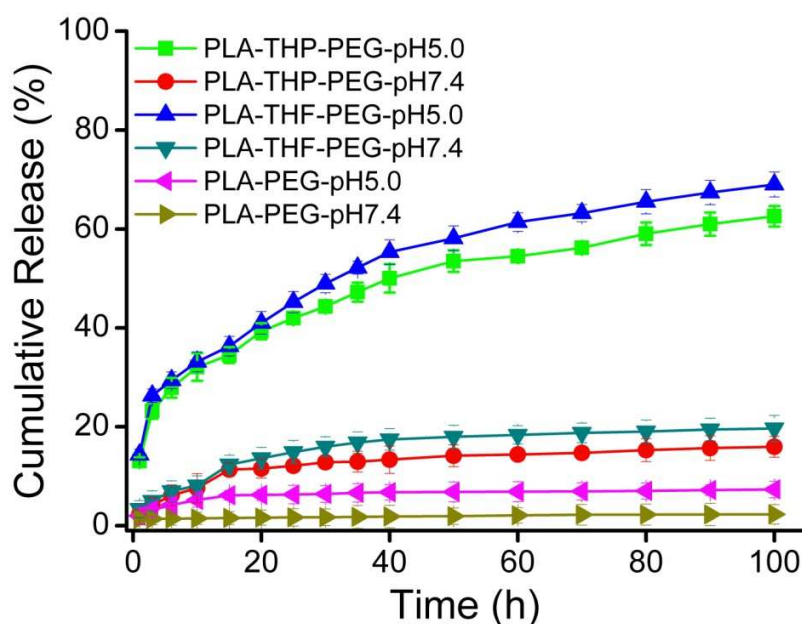


Figure 5 DOX release profiles of DOX-loaded PLA-THF-PEG **18c**, PLA-THP-PEG **4d** and PLA-PEG micelles at 37 °C in pH 5.0 and pH 7.4, respectively

3.6. Confocal Microscopy Studies

CLSM was exploited to further investigate and compare the cell uptake behavior and intracellular distribution of the DOX loaded micelles with that of free DOX by HeLa cells. Prior to the incubation of HeLa cells at 37 °C for predetermined interval 60 min, both of DOX loaded PLA-THP-PEG and PLA-THF-PEG micelles were added to culture medium with a DOX concentration of 9 $\mu\text{g}/\text{mL}$. Stained with DAPI, the nuclei and cytoplasm of pretreated cells were observed by CLSM. By comparison with the control in Figure 6A, the observation reveals that free DOX is largely accumulated in the cell nuclei of HeLa cells in Figure 6B, while DOX released from DOX loaded micelles is mainly located in the cytoplasm in Figure 6C and 6D. The result also indicates that free DOX is

taken up by diffusion through the cell membrane and the DOX loaded micelles are taken up by the cells via the endocytosis process. CLSM analyses confirmed that the DOX loaded micelles can be efficiently internalized by the HeLa cells.

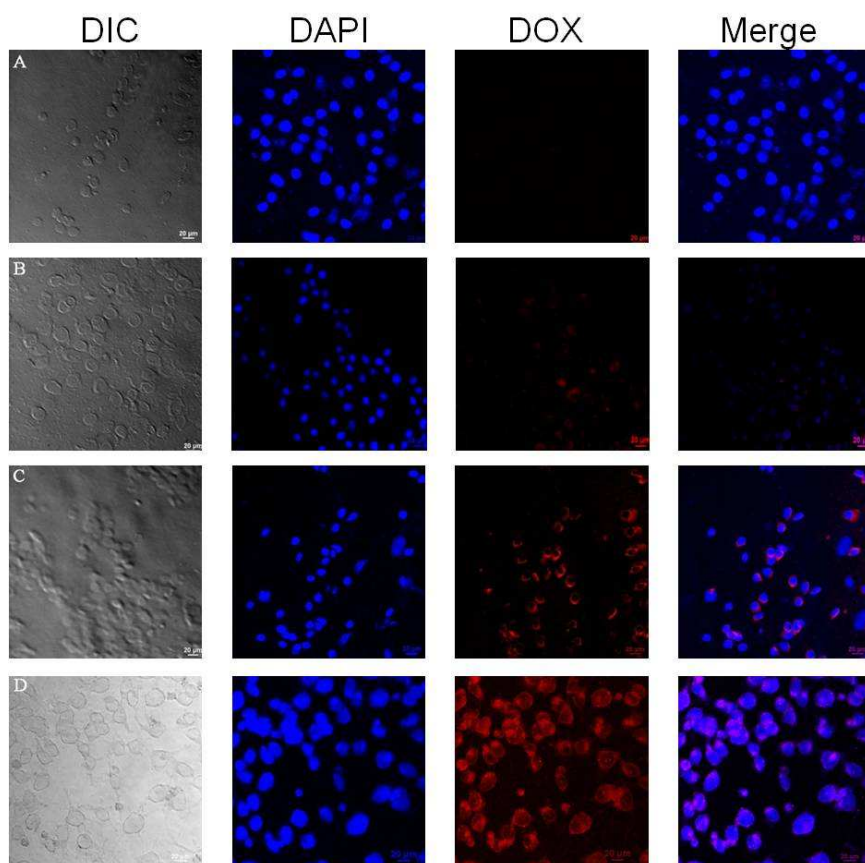


Figure 6 CLSM images of HeLa cells incubated with (A) neither free DOX nor DOX-loaded micelles (B) free DOX, (C) DOX-loaded PLA-THP-PEG **4d** micelles and (D) DOX-loaded PLA-THP-PEG **18c** micelles at 37 °C for 60 min; Cell nuclei were stained with DAPI.

3.7. Activity Analysis of the Drug-Loaded Micelles

The drug loaded self-assembled micelles were further investigated to evaluate the potential therapeutic efficacy. The in vitro cytotoxicity of DOX-loaded PLA-THP-PEG

and PLA-THF-PEG micelles compared with that of free DOX was determined by MTT assay against HeLa cells. To analyze the activity of DOX loaded nanoparticles, HeLa cells were cultured in the solutions of free DOX and DOX loaded micelles at different DOX concentrations ranging from 0.5 to 10 $\mu\text{g}/\text{mL}$ for 48h, respectively. As shown in Figure 7, the viability of HeLa cells depends on DOX concentration. It can be found that DOX loaded micelles perform potent effect of inhibition to HeLa cell proliferation similar to free DOX. The inhibition of cancer cell growth is attributed to the intracellular DOX released from the DOX loaded micelles and final entry into the nuclei of HeLa cells. Moreover, the DOX loaded PLA-THF-PEG and PLA-THF-PEG micelles and free DOX doses required for 50% cellular growth inhibition (IC_{50}) are 2.08, 2.14 and 0.83 mg/mL , respectively. Both of the DOX loaded micelles show slightly lower cytotoxicity than free DOX due to the time-consuming DOX release from DOX loaded micelles in comparison to free DOX at the same DOX concentration, proved by the in vitro DOX release. The result reveals that DOX released from the micelles could exploit a potent drug efficacy as free DOX after entry into the HeLa cells, producing the desired pharmacological action and minimizing the side effect of free DOX.

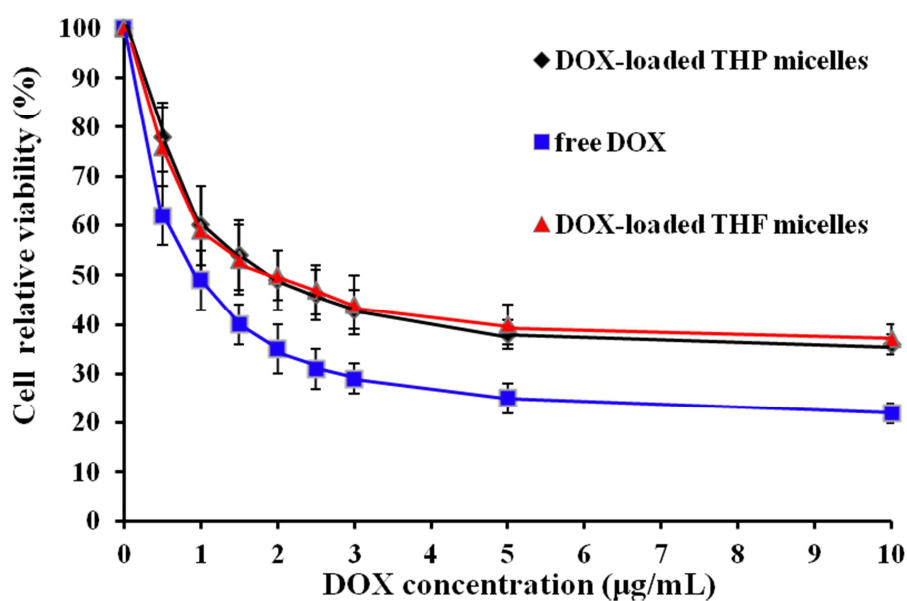


Figure 7 *In vitro* cell viability of HeLa cells against free DOX and DOX-loaded THP and THF micelles (**4d** and **18c**) at different concentrations

4. Conclusions

In conclusion, the paper constructed an acid sensitive drug delivery system based on amphiphilic PLA-THP-PEG and PLA-THF-PEG diblock copolymers. The obtained diblock copolymers were characterized by ^1H NMR and GPC, their self assembled micelles exhibited unimodal size distribution, with mean diameters ranging from 19 nm to 53 nm. Their average size of DOX-loaded micelles **4d** and **18c** increased compared with that of blank micelles. The CMC of every diblock copolymers is in the range of 10^{-6} M, indicated the high stability of polymeric micelles. Further study confirmed that the micelles kept stable up to 35 days under physiological conditions. Both of the PLA-THP-PEG and PLA-THF-PEG polymeric micelles showed accelerated drug release at pH 5.0 compared with that at pH 7.4. Under the same conditions the release rate of micelles with THF linkage is faster than that owns THP linkage. Moreover the copolymer

micelles without acid sensitive linkage kept stable even in acidic conditions which indicated that the THP and THF linkage plays important role in drug release. The in vitro cell assay demonstrated that DOX-loaded PLA-THP-PEG and PLA-THF-PEG micelles are able to enter the cells and produce the desired pharmacological action as that of free DOX. Confocal microscopy studies indicated that the DOX-loaded PLA-THP-PEG and PLA-THF-PEG micelles performed good cell internalization. In one word, the strategy for employing THP and THF linkage in the formation of acid sensitive block copolymer micelles provides a potential alternative for pH-responsive drug delivery system.

Acknowledgement

We acknowledge the financial supports provided by the National Natural Science Foundation of China (81071250 and 91227109), Major Projects in National Science and Technology, “Creation of Major New Drugs” (2011ZX09501-001-05), and the US National Science Foundation (CHE-1306326).

Supplementary material

Supplementary data related to this article can be found at

<http://dx.doi.org/10.1016/j.polymer>

References

- [1] Wei H, Zhuo R-X, Zhang X-Z. *Progress in Polymer Science* 2013;38:503-35.
- [2] Ryu J-H, Roy R, Ventura J, Thayumanavan S. *Langmuir* 2010;26:7086-92.
- [3] Kataoka K, Harada A, Nagasaki Y. *Advanced Drug Delivery Reviews* 2012;64:37-48.
- [4] Li C, Liu S. *Chemical Communications* 2012;48:3262-78.
- [5] Torchilin V. *European Journal of Pharmaceutics and Biopharmaceutics* 2009;71:431-44.
- [6] Mura S, Nicolas J, Couvreur P. *Nature Materials* 2013;12:991-1003
- [7] Choi KY, Jeon EJ, Yoon HY, Lee BS, Na JH, Min KH, et al. *Biomaterials* 2012;33:6186-93.
- [8] Murakami M, Cabral H, Matsumoto Y, Wu S, Kano MR, Yamori T, et al. *Science Translational Medicine* 2011;3:64ra2-ra2.

- [9] Stuart MAC, Huck WTS, Jan Genzer, Müller M, Ober C, Stamm M, Sukhorukov GB, Szleifer I, Tsukruk VV, Urban M, Winnik F, Zauscher S, Iuzinov I, Minko S. Nature Materials 2010;9:101-13.
- [10] Khoee S, Hemati K. Polymer 2013;54:5574-5585.
- [11] Bhatt S, Pulpytel J, Mirshahi M, and Arefi-Khonsari F. Polymer 2013;54:4820-4829.
- [12] Gupta S, Tyagi R, Parmar VS, Sharma SK, and Haag R. Polymer 2012;53:3053-3078.
- [13] Hubbell JA. Science 2003;300:595-6.
- [14] Amstad E, Kim S-H, Weitz DA. Angewandte Chemie International Edition 2012;51:12499-503.
- [15] Wang F, Klaukherd A, Thayumanavan S. Journal of the American Chemistry Society 2011;133:13496-503.
- [16] Wennink JWH, Signori F, Karperien M, Bronco S, Feijen J, and Dijkstra PJ. Polymer 2013;54:6894-6901.
- [17] Zhang CY, Yang YQ, Huang TX, Zhao B, Guo XD, Wang JF, et al. Biomaterials 2012;33:6273-83.
- [18] Cai G, Zhang H, Liu P, Wang L, Jiang H. Acta Biomaterialia 2011;7:3729-37.
- [19] Du Y, Chen W, Zheng M, Meng F, Zhong Z. Biomaterials 2012;33:7291-9.
- [20] Du JZ, Du XJ, Mao CQ, Wang J. Journal of the American Chemistry Society 2011;133:17560-3.
- [21] Kim H, Kang YJ, Jeong ES, Kang S, Kim KT. ACS Macro Lett 2012;1:1194-8.

- [22] Yin L, Dalsin MC, Sizovs A, Reineke TM, Hillmyer MA. *Macromolecules* 2012;45:4322-32.
- [23] Khorsand B, Lapointe G, Brett C, Oh JK. *Biomacromolecules* 2013;14:2103-11.
- [24] Thambi T, Deepagan VG, Ko H, Lee DS, Park JH. *Journal of Materials Chemistry* 2012; 22: 22028-36.
- [25] Feng F, Li R, Zhang Q, Wang Y, Yang X, Duan H, and Yang X. *Polymer* 2014;55:110-118.
- [26] Lee J-E, Ahn E, Bak JM, Jung S-H, Park JM, Kim B-S, and Lee H-i. *Polymer* 2014;55:1436-1442.
- [27] Chen C-J, Jin Q, Liu G-Y, Li D-D, Wang J-L, and Ji J. *Polymer* 2012;53:3695-3703.
- [28] Xu Y, Ma R, Zhang Z, He H, Wang Y, Qu A, An Y, Zhu XX, and Shi L. *Polymer* 2012;53:3559-3565.
- [29] Topuzogullari M, Bulmus V, Dalgakiran E, and Dincer S. *Polymer* 2014;55:525-534.
- [30] Klinger D and Landfester K. *Polymer* 2012;53:5209-5231.
- [31] Cajot S, Van Butsele K, Paillard A, Passirani C, Garcion E, Benoit JP, et al. *Acta Biomaterialia* 2012;8:4215-23.
- [32] Dadsetan M, Taylor KE, Yong C, Bajzer Ž, Lu L, Yaszemski MJ. *Acta Biomaterialia* 2013;9:5438-46.
- [33] Zhang Z, Chen X, Chen L, Yu S, Cao Y, He C, et al. *ACS Applied Materials & Interfaces* 2013;5:10760-6.

- [34] Qiu L, Li Z, Qiao M, Long M, Wang M, Zhang X, et al. *Acta Biomaterialia* 2013.
- [35] Lin W, Kim D. *Langmuir* 2011; 27: 12090-7.
- [36] Ian FT, Daniela R. *Cancer Research* 1989;49:4373-84.
- [37] Cui W, Qi M, Li X, Huang S, Zhou S, Weng J. *International Journal of Pharmaceutics* 2008;361:47-55.
- [38] Huang X. *Macromolecules* 2009;42:783-90.
- [39] Zhou L, Yu L, Ding M, Li J, Tan H, Wang Z, et al. *Macromolecules* 2011;44:857-64.
- [40] Prabakaran M, Grailer JJ, Pilla S, Steeber DA, Gong S. *Biomaterials* 2009;30:5757-66.
- [41] Akter S, Clem BF, Lee HJ, Chesney J, Bae Y. *Pharmaceutical Research* 2012;29:847-55.
- [42] Jackson AW, Stakes C, Fulton DA. *Polymer Chemistry* 2011;2:2500-11.
- [43] Srinophakun T, Boonmee J. *International Journal of Molecular Sciences* 2011;12:1672-83.
- [44] Jin Y, Song L, Su Y, Zhu LJ, Pang Y, Qiu F, Tong GS, Yan DY, Zhu BS, Zhu XY. *Biomacromolecules* 2011;12:3460-8.
- [45] Klaikherd A, Nagamani C, Thayumanavan S. *Journal of the American Chemistry Society* 2009;131:4830-38.
- [46] Elizabeth R. Gillies APG, and Jean M. J. Fréchet. *Bioconjugate Chemistry* 2004;15:1254-63.

- [47] Alexandridis P, Holzwarth J. F, Hatton TA. *Macromolecules* 1994;27:2414-25.
- [48] Adams ML, Lavasanifar A, Kwon GS. *Journal of Pharmaceutical Sciences* 2003;92:1343-55.
- [49] Torchilin VP. *Journal of Control Release* 2001;73:137-172.
- [50] Nishiyama N, Kataoka K. *Pharmacology & Therapeutics* 2006;112:630-48.
- [51] Xu XY, Zhang SF, Wang XH, Li YX, Jing X B. *Polymers for Advanced Technologies* 2009;20:843-48.
- [52] Wang DL, Su Y, Zhu BS, Pang Y, Zhu LJ, Liu JY, Tu CL, Yan DY, Zhu XY. *Biomacromolecules* 2011;12:1370-9.
- [53] Young CR, Dietzsch C, Cerea M, Farrell T, Fegely KA, Rajabi-Siahboomi A, et al. *International Journal of Pharmaceutics* 2005;301:112-20.

Supplementary material**Self-assembled Polymeric Micelles Based on THP and THF Linkage for pH-Responsive Drug Delivery**

Fangxia Zhu[†], Qinglai Yang[†], Yuan Zhuang[†], Yuanqing Zhang[‡], Zhifeng Shao[‡], Bing Gong^{||,§,*} and Yu-Mei Shen^{†,*}

[†]Shanghai Center for Systems Biomedicine, Key Laboratory of Systems Biomedicine and Bio-ID Center, Shanghai Jiao Tong University, Shanghai 200240, China

[‡]Shanghai Institute of Applied Physics, Chinese Academy of Sciences, Shanghai 201800, China

[‡]State Key Laboratory of Oncogenes and Bio-ID Center, School of Biomedical Engineering, Shanghai Jiao Tong University, Shanghai 200240, China

^{||}College of Chemistry, Beijing Normal University, Beijing 100875, China

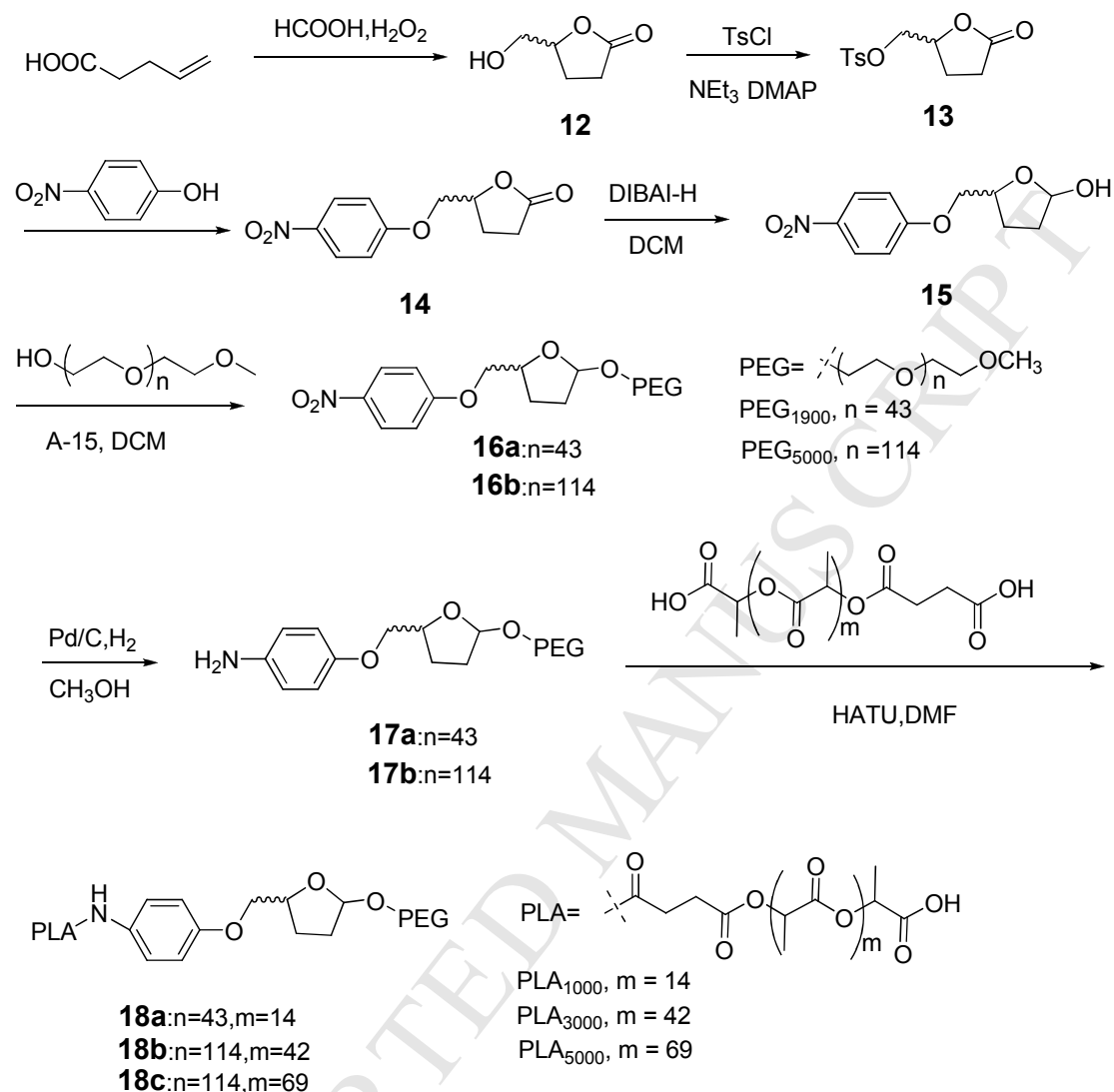
[§]Department of Chemistry, University at Buffalo, State University of New York, Buffalo, NY 14260, United States

E-mail: yumeishen@sjtu.edu.cn; bgong@buffalo.edu

Contents

1. Synthesis of PLA-THF-PEG Copolymers	3
2. Copies of ^1H-NMR and ^{13}C-NMR spectrum	8
3. FT-IR Spectra	16
4. GPC Curves of Block Copolymers	21
5. Preparation of PLA-THP-PEG and PLA-THF-PEG Micelles	22

1. Synthesis of PLA-THF-PEG copolymers



Scheme S1 Synthesis of diblock copolymers PLA-THF-PEG

20 mL 88% formic acid and 7.7 mL 30% hydrogen peroxide were added to flask and stirred at 50 °C. Then 5.01 g 4-pentenoic acid (50 mmol) was dissolved in 10 mL 88% formic acid and dropwise added to the flask (in 15 min). The reaction was continued to stir at 50 °C for 10 hrs, then the solvent was evaporated and added 0.35 mL concentrated hydrochloric acid and 17 mL dry methanol, stirred at room temperature for 4 hrs, then the reaction was evaporated and pure yellow liquid **12** was obtained. Yield: 5.8 g, 100%. ¹H NMR (CDCl₃, 400 MHz): δ 4.65-4.56 (m, 1H),

3.89-3.81 (m, 1H), 3.65-3.57 (m, 1H), 2.65-2.45 (m, 2H), 2.30-2.18 (m, 1H), 2.18-2.06 (m, 1H).

6.6 g compound **12** (56.9 mmol) was dissolved in 80 mL DCM, then added 10 mL triethylamine, 560 mg dimethylamino pyridine (DMAP) (4.6 mmol) and 10.86 g TsCl (56.9 mmol), stirred for 4 hrs at room temperature. The reaction was stopped and the organic extract washed with water, brine, dried over with anhydrous sodium sulfate, and the filtrate was evaporated to give a solid. Column chromatography (PE: DCM = 2:1, 1:2), to give pure product **13**. Yield: 13.5 g, 87.7%. ¹H NMR (CDCl₃, 400 MHz): δ 7.78 (d, J = 8.4 Hz, 2H), 7.36 (d, J = 8.4 Hz, 2H), 4.72-4.65 (m, 1H), 4.21-4.11 (m, 2H), 2.64-2.48 (m, 2H), 2.45 (s, 3H), 2.40-2.30 (m, 1H), 2.17-2.07 (m, 1H). ¹³C NMR (100 MHz, CDCl₃): δ 176.1, 145.5, 132.3, 130.2, 128.1, 76.5, 70.1, 28.0, 23.6, 21.8. IR (KBr): 3437, 2924, 1779, 1598, 1495, 1458, 1358, 1266, 1190, 1176, 1095, 1003, 957, 860, 812, 740, 665, 569, 554.

9.057 g compound **13** (33.5 mmol) and 5.09 g K₂CO₃ (36.8 mmol) were added to flask, 6.65 g 4-nitrophenol (47.8 mmol) was dissolved in 60 mL DMF and added to the flask. Under nitrogen atmosphere, the reaction was placed in an oil bath at 80 °C for stirring for 5 hrs. Then the reaction was stopped and extracted with CH₂Cl₂, the combined organic extracts were washed with water and brine, dried over anhydrous magnesium sulfate (MgSO₄), filtered, followed by removing solvent. Pure product **14** as yellow solid was obtained by column chromatography. Yield: 7.67 g, 95.8%. ¹H NMR (CDCl₃, 400 MHz): δ 8.13 (d, J = 9.2 Hz, 2H), 6.94 (d, J = 9.2 Hz, 2H), 4.94-4.86 (m, 1H), 4.31-4.26 (m, 1H), 4.19-4.13 (m, 1H), 2.73-2.54 (m, 2H),

2.49-2.39 (m, 1H), 2.29-2.19 (m, 1H). ^{13}C NMR (100 MHz, CDCl_3): δ 176.9, 163.1, 142.0, 125.9, 114.6, 69.9, 28.3, 23.8. IR (KBr): 3446, 2924, 1771, 1647, 1607, 1593, 1557, 1542, 1509, 1497, 1456, 1384, 1340, 1298, 1261, 1160, 1111, 1073, 983, 944, 919, 846, 751, 689, 668.

Under nitrogen atmosphere, 6 g compound **14** (25.3 mmol) was dissolved in 40 mL CH_2Cl_2 and stirred at $-78\text{ }^\circ\text{C}$, then slowly added 20 mL diisobutylaluminum hydride (DIBAL-H) (1.5 M in Toluene, 30 mmol) to the reaction. After stirring for 4 hrs, the reaction was stopped. Extracted with CH_2Cl_2 , the combined organic extracts were washed with water and brine, dried over anhydrous magnesium sulfate (MgSO_4), filtered, the solvent was evaporated under reduced pressure to give desire product **15**. Yield: 4.1 g, 67%. ^1H NMR (CDCl_3 , 400 MHz): δ 8.21-8.16 (m, 2H), 7.01-6.95 (m, 2H), 5.65-5.55 (m, 1H), 4.67-4.60 (m, 1H), 4.16-4.13 (m, 1H), 4.10-4.00 (m, 1H), 2.32-2.03 (m, 2H), 2.02-1.76 (m, 2H). ^{13}C NMR (100 MHz, CDCl_3): δ 163.7, 141.9, 126.1, 114.7, 72.9, 69.9, 62.9, 30.6, 28.9. IR (KBr): 3411, 3115, 3084, 2929, 1607, 1593, 1510, 1453, 1342, 1299, 1264, 1174, 1112, 1070, 1025, 967, 890, 847, 752, 691, 650, 500.

729 mg compound **15** (3 mmol), PEG (1.5 mmol) and 600 mg Amberlyst A-15 was dissolved in 80 mL toluene and refluxed at $100\text{ }^\circ\text{C}$ for 10 hrs. The reaction solution was removed by filtration through Celite to give a yellow solid. Pure product **16** was obtained by column chromatography.

16a, yield: 42.6%. ^1H NMR (CDCl_3 , 400 MHz): δ 8.18-8.13 (m, 2H), 6.99-6.92 (m, 2H), 5.22-5.12 (m, 1H), 4.49-4.40 (m, 1H), 4.14-3.97 (m, 2H), 3.87-3.39 (m,

195H), 3.34 (s, 4H), 2.22-1.70 (m, 4H). IR (KBr): 3446, 2920, 2867, 1647, 1592, 1509, 1456, 1384, 1341, 1260, 1108, 950, 850, 669.

16b, yield: 23.7%. ^1H NMR (CDCl_3 , 400 MHz): δ 8.21-8.17 (m, 2H), 7.02-6.96 (m, 2H), 5.25-5.16 (m, 1H), 4.51-4.45 (m, 1H), 4.16-4.06 (m, 2H), 3.89-3.43 (m, 372H), 3.37 (s, 3H), 2.12-1.96 (m, 4H). IR (KBr): 3446, 2923, 2853, 1632, 1508, 1456, 1384, 1640, 1246, 1091, 931, 837, 752, 669.

Under hydrogen atmosphere, 1.8 g compound **16** and 360 mg 10% Pd / C was dissolved in 45 mL methanol. The mixture was stirred at 35 °C for 12 h and the reaction solvent was filtered, evaporated to give yellow solid **17**.

17a, yield: 89.1%. ^1H NMR (CDCl_3 , 400 MHz): δ 6.70-6.60 (m, 2H), 6.56-6.42 (m, 2H), 5.20-5.09 (m, 1H), 4.42-4.30 (m, 1H), 3.90-3.80 (m, 2H), 3.80-3.41 (m, 170H), 3.33 (s, 3H), 2.18-1.64 (m, 4H). IR (KBr): 3445, 2952, 2923, 2868, 1635, 1510, 1457, 1377, 1348, 1296, 1239, 1100, 948, 851, 669.

17b, yield: 80.3%. ^1H NMR (CDCl_3 , 400 MHz): δ 6.88-6.70 (m, 4H), 5.22-5.10 (m, 1H), 4.45-4.36 (m, 1H), 3.97-3.85 (m, 2H), 3.89-3.40 (m, 403H), 3.35 (s, 3H), 2.17-1.91 (m, 4H). IR (KBr): 3446, 2954, 2859, 1647, 1509, 1456, 1384, 1348, 1246, 1100, 947, 669.

Under nitrogen atmosphere, PLA (1 mmol) and HATU (2 mmol) were dissolved in 30 mL DMF, then DIPEA (1 mmol) was added and the reaction was stirred at 0 °C for 0.5 hr. After adding **17** (0.5 mmol, dissolved in 4 mL DMF) the reaction was stirred at 30 °C for an additional 30 hrs. The resulting mixture was poured into a few drops of concentrated hydrochloric acid and extracted with CH_2Cl_2 . The combined

organic extracts were washed with water and brine, dried over anhydrous magnesium sulfate, filtered, and the filtrate was evaporated. Purification was accomplished by chromatography to give the desired product **18**.

18a, yield: 63.8%. ^1H NMR (CDCl_3 , 400 MHz): δ 7.51-7.36 (m, 2H), 6.88-6.76 (m, 2H), 5.35-5.26 (m, 1H), 5.22-5.05 (m, 11H), 4.45-4.37 (m, 1H), 3.99-3.89 (m, 2H), 3.84-3.40 (m, 156H), 3.34 (s, 3H), 2.80-2.40 (m, 4H), 2.21-1.79 (m, 4H), 1.64-1.40 (m, 34H). IR (KBr): 3446, 2921, 2852, 1747, 1647, 1509, 1454, 1349, 1187, 1090, 946, 840, 669.

18b, yield: 32.6%. ^1H NMR (CDCl_3 , 400 MHz): δ 7.55-7.36 (m, 2H), 6.85-6.65 (m, 2H), 5.35-5.26 (m, 1H), 5.22-5.05 (m, 29H), 4.43-4.37 (m, 1H), 3.99-3.85 (m, 2H), 3.84-3.40 (m, 406H), 3.33 (s, 3H), 2.78-2.52 (m, 4H), 2.13-1.84 (m, 4H), 1.64-1.40 (m, 93H). IR (KBr): 3446, 2921, 2855, 1748, 1647, 1509, 1455, 1348, 1275, 1260, 1185, 1091, 946, 860, 764, 750.

18c, yield: 19.7%. ^1H NMR (CDCl_3 , 400 MHz): δ 7.54-7.37 (m, 2H), 6.90-6.72 (m, 2H), 5.35-5.26 (m, 2H), 5.22-5.05 (m, 26H), 4.45-4.39 (m, 1H), 4.09-3.86 (m, 2H), 3.84-3.40 (m, 396H), 3.35 (s, 3H), 2.78-2.57 (m, 6H), 2.18-1.86 (m, 9H), 1.64-1.40 (m, 83H). IR (KBr): 3502, 2934, 2870, 1756, 1541, 1511, 1455, 1351, 1256, 1187, 1098, 951, 862, 750.

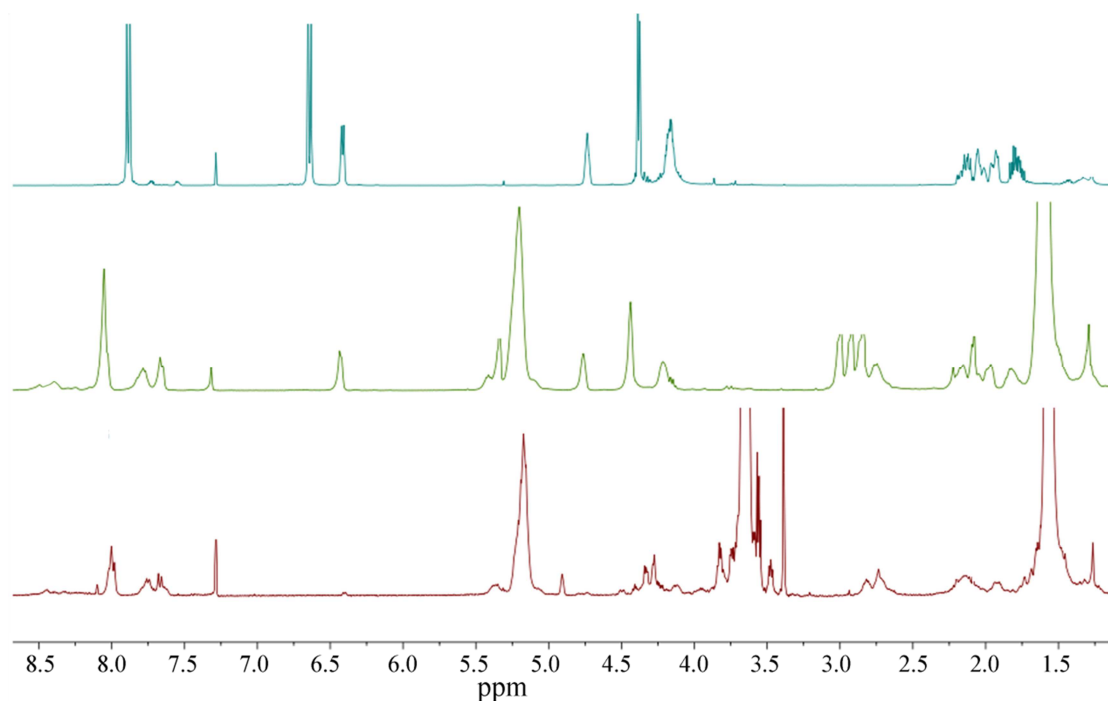
2. Copies of ^1H -NMR and ^{13}C -NMR

Figure S1. ^1H -NMR spectra of intermediate **2**, intermediate **3a** ($m = 14$) and terminal product **4a** (400 MHz, CDCl_3).

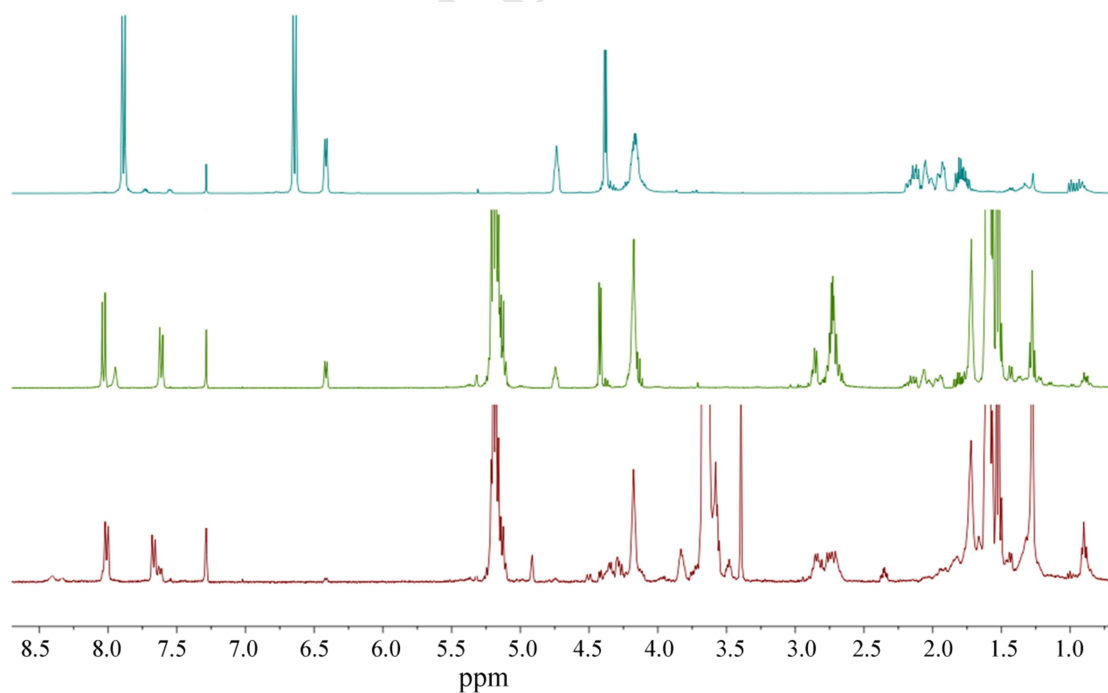


Figure S2. ^1H -NMR spectra of intermediate **2**, intermediate **3b** ($m = 42$) and the

terminal product **4b** (400 MHz, CDCl₃).

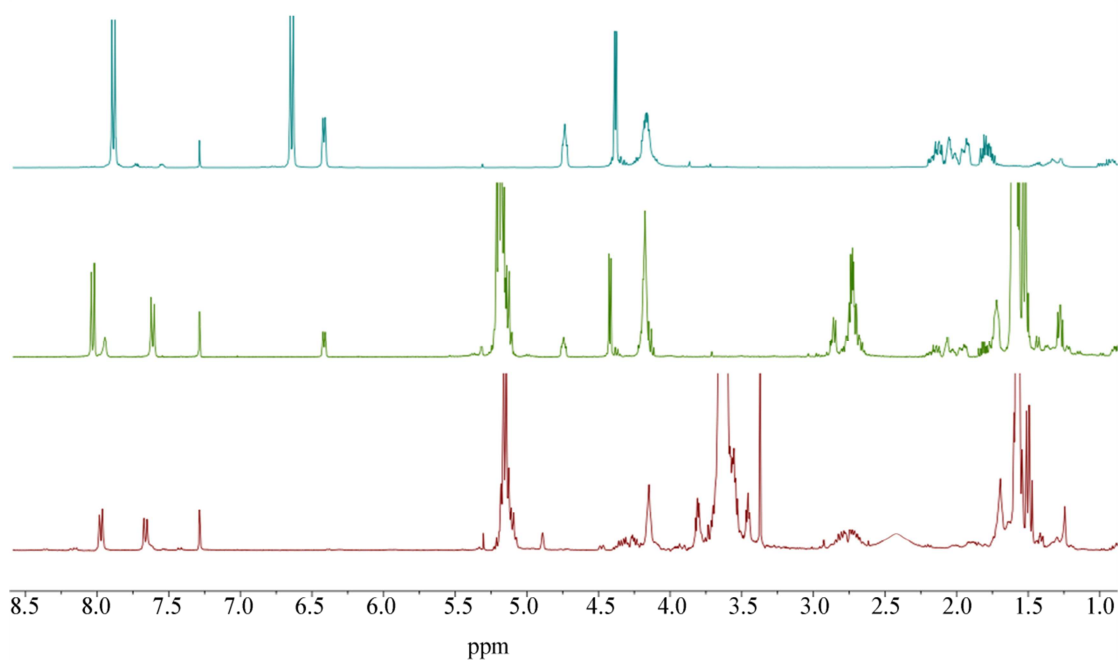


Figure S3. ¹H-NMR spectra of intermediate **2**, intermediate **3b** (m = 42) and terminal product **4c** (400 MHz, CDCl₃).

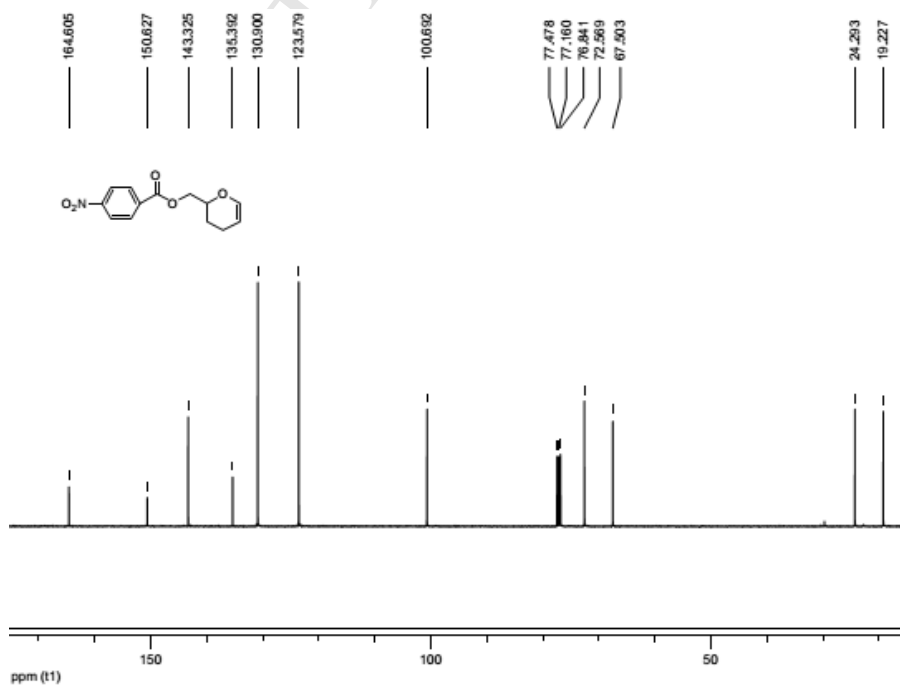
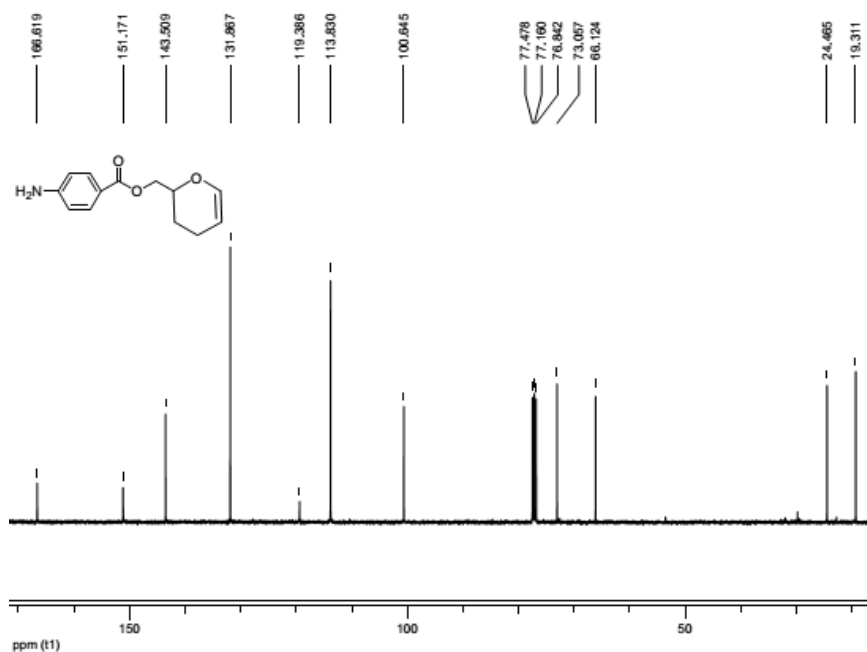
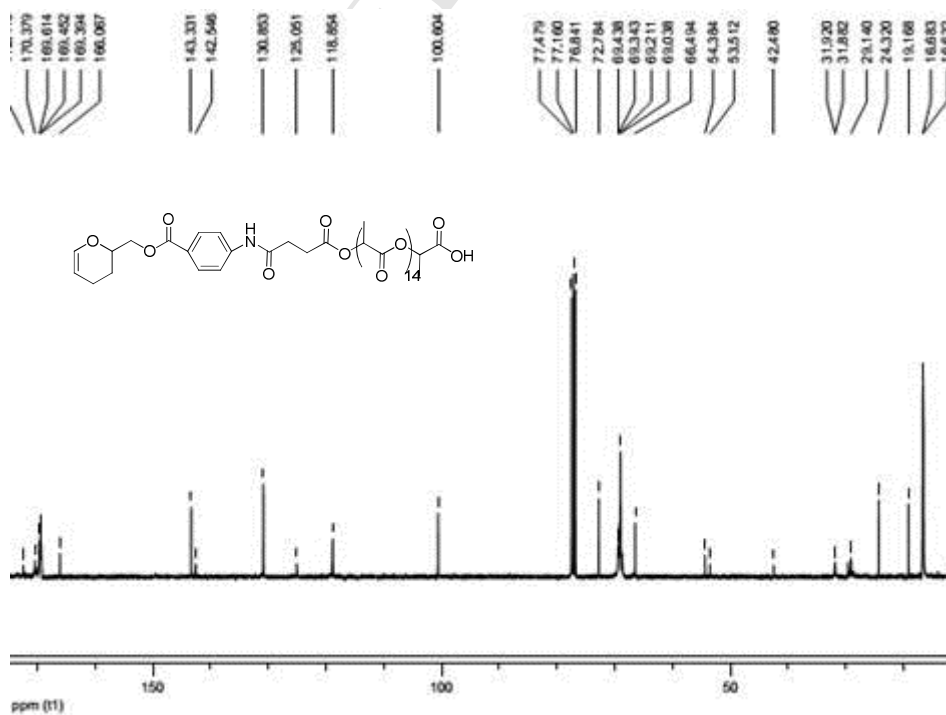


Figure S4. ^{13}C -NMR spectrum of intermediate **1** (100 MHz, CDCl_3)**Figure S5.** ^{13}C -NMR spectrum of intermediate **2** (100 MHz, CDCl_3)**Figure S6.** ^{13}C -NMR spectrum of intermediate **3a** (100 MHz, CDCl_3)

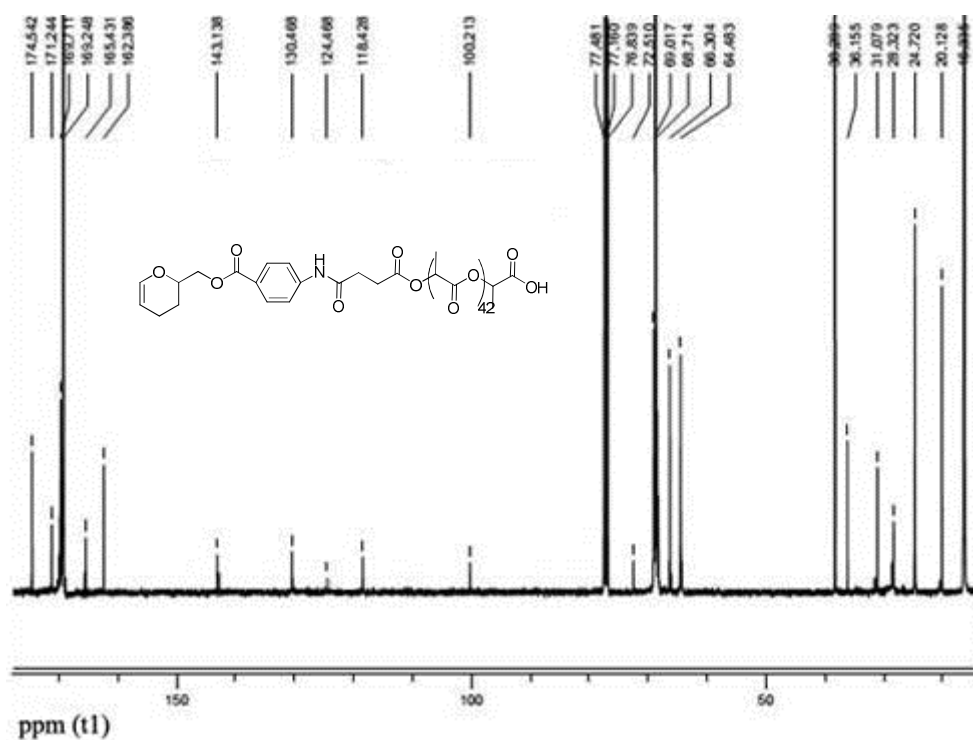


Figure S7. ¹³C-NMR spectrum of intermediate **3b** (100 MHz, CDCl₃)

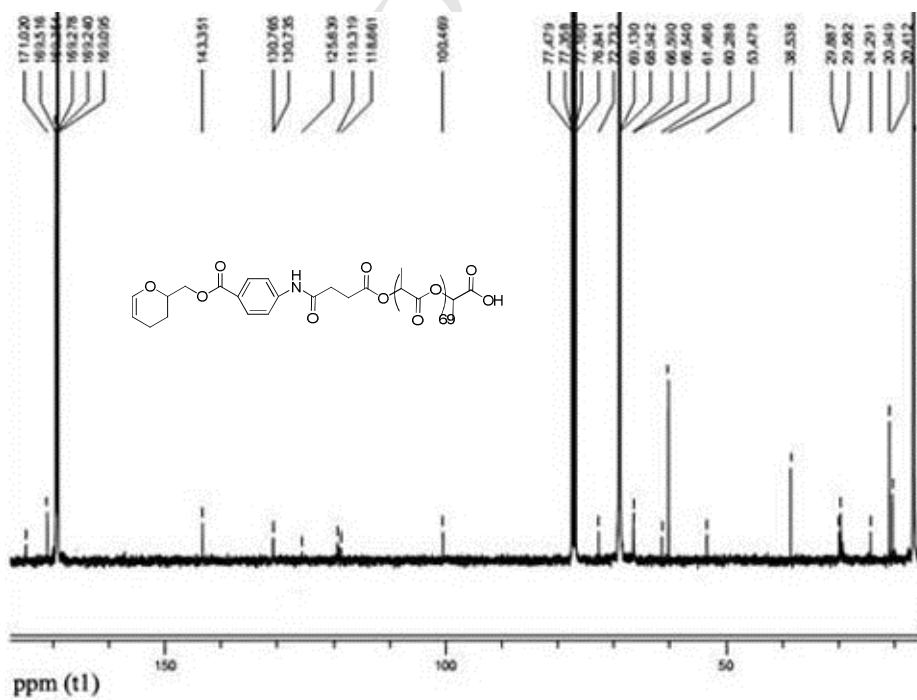


Figure S8. ¹³C-NMR spectrum of intermediate **3c** (100 MHz, CDCl₃)

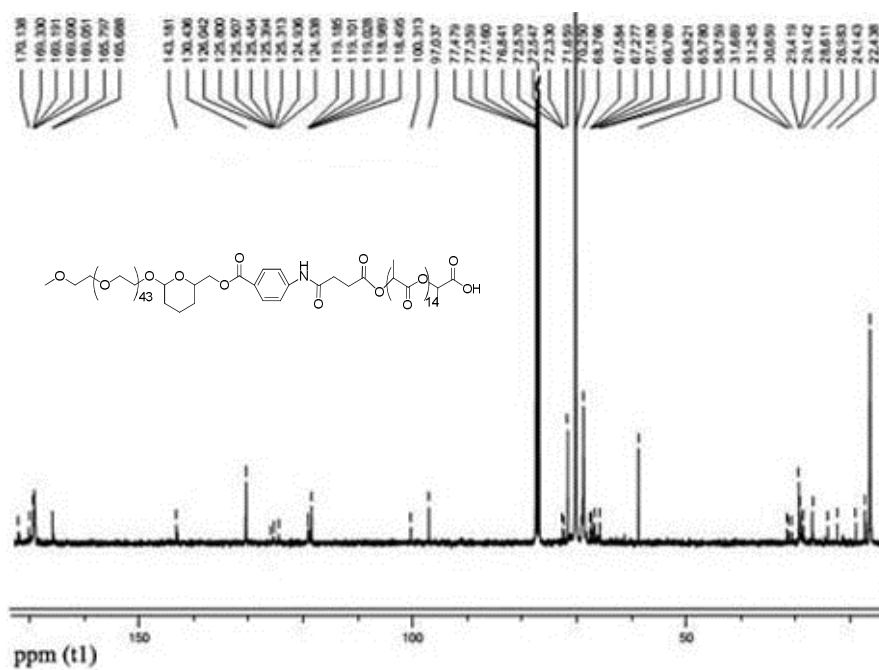


Figure S9. ^{13}C -NMR spectrum of terminal product **4a** (100 MHz, CDCl_3)

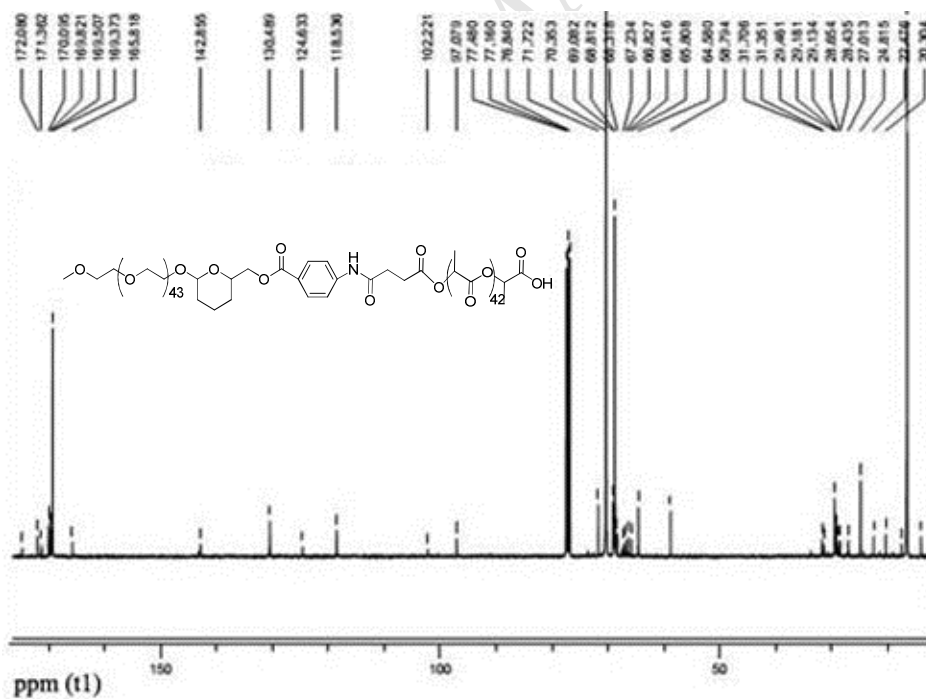


Figure S10. ^{13}C -NMR spectrum of intermediate **4b** (100 MHz, CDCl_3)

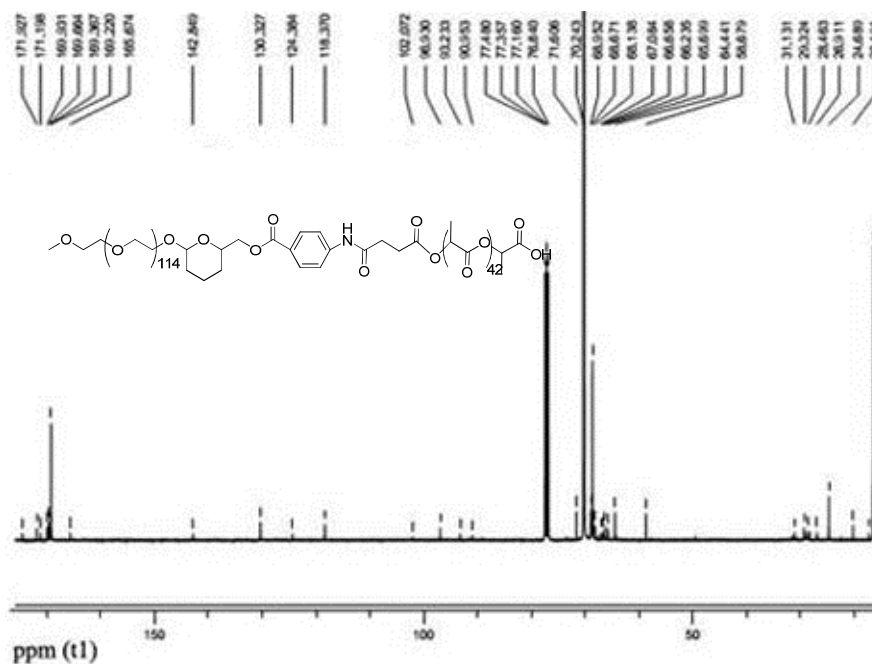


Figure S11. ¹³C-NMR spectrum of intermediate **4c** (100 MHz, CDCl₃)

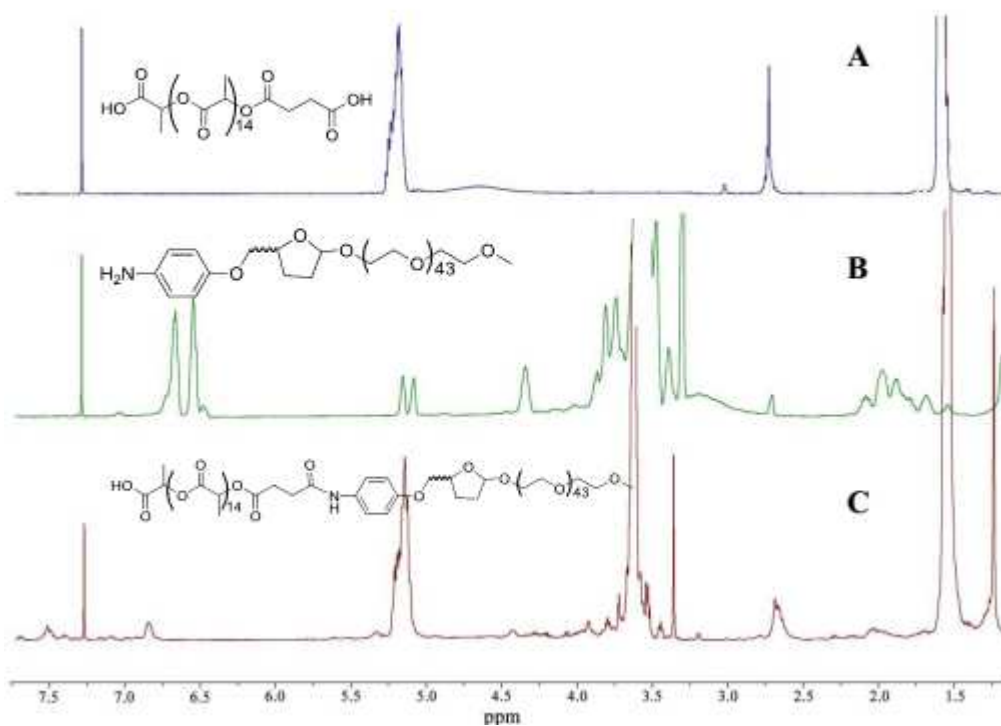


Figure S12. ¹H-NMR spectra of PLA₃₀₀₀, **17a** and **18a** (400 MHz, CDCl₃)

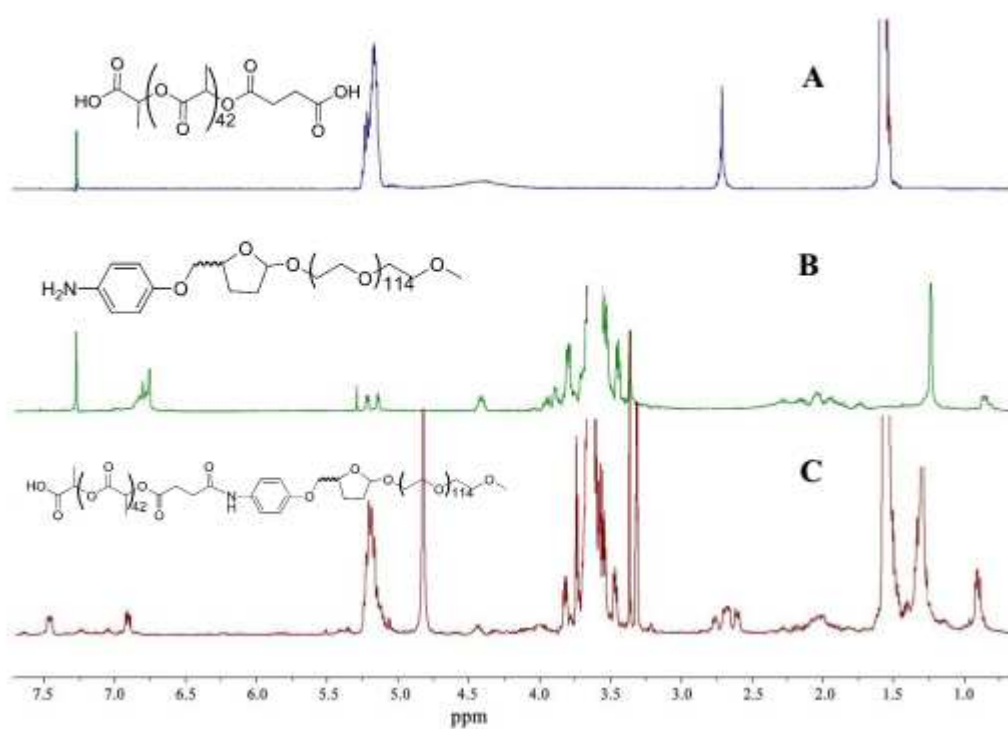


Figure S14. $^1\text{H-NMR}$ spectra of PLA_{5000} , **17b** and **18b** (400 MHz, CDCl_3)

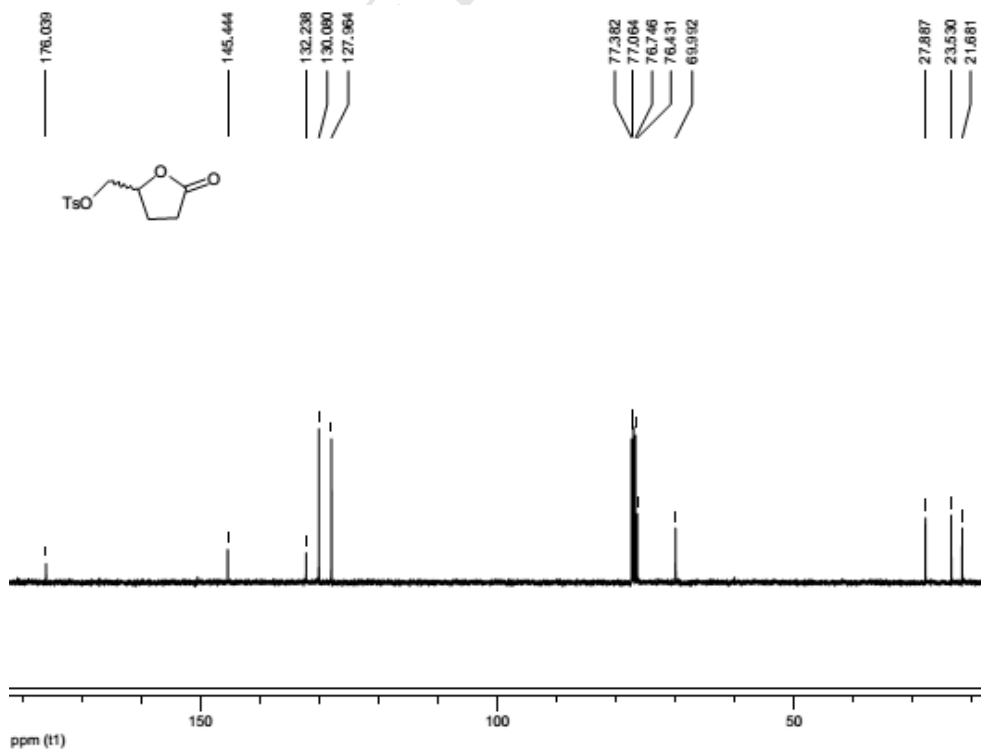
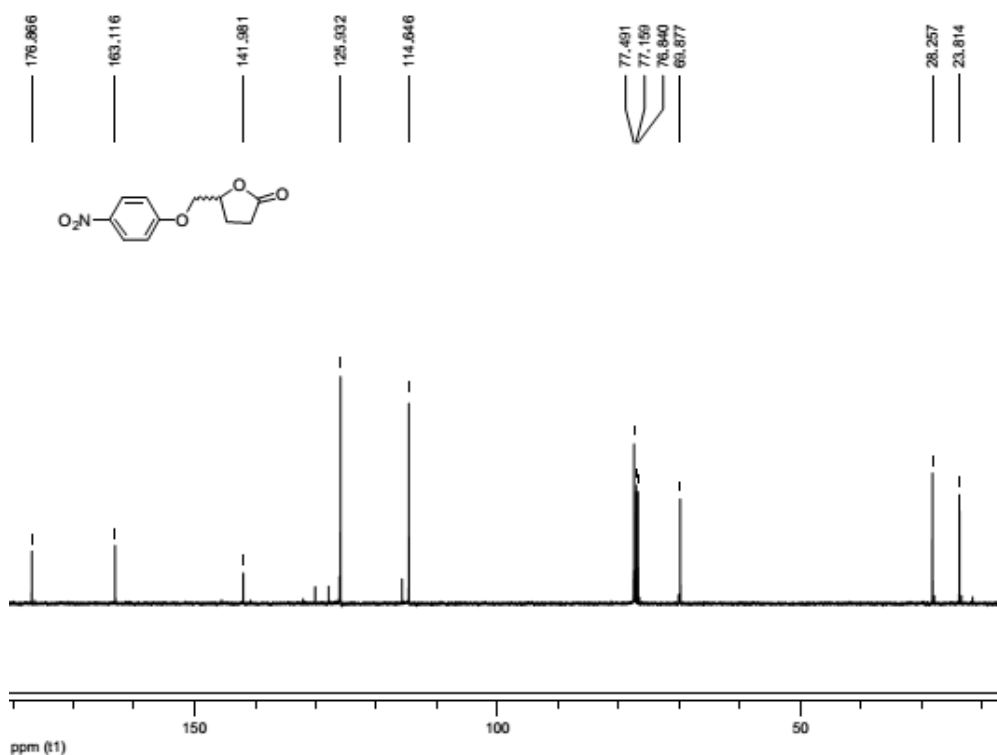
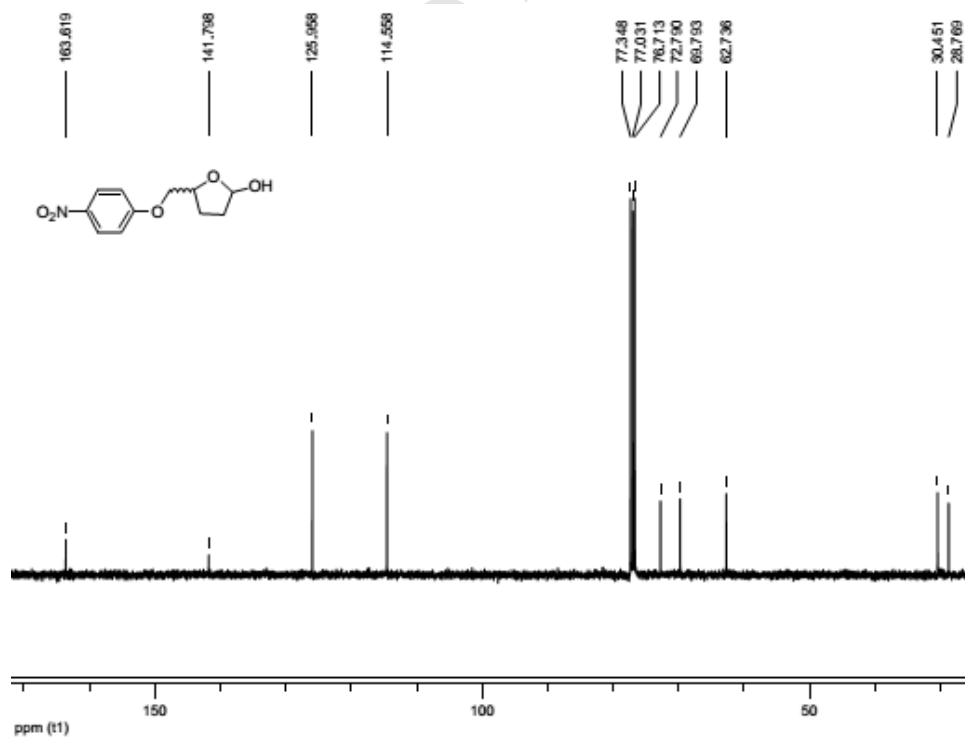
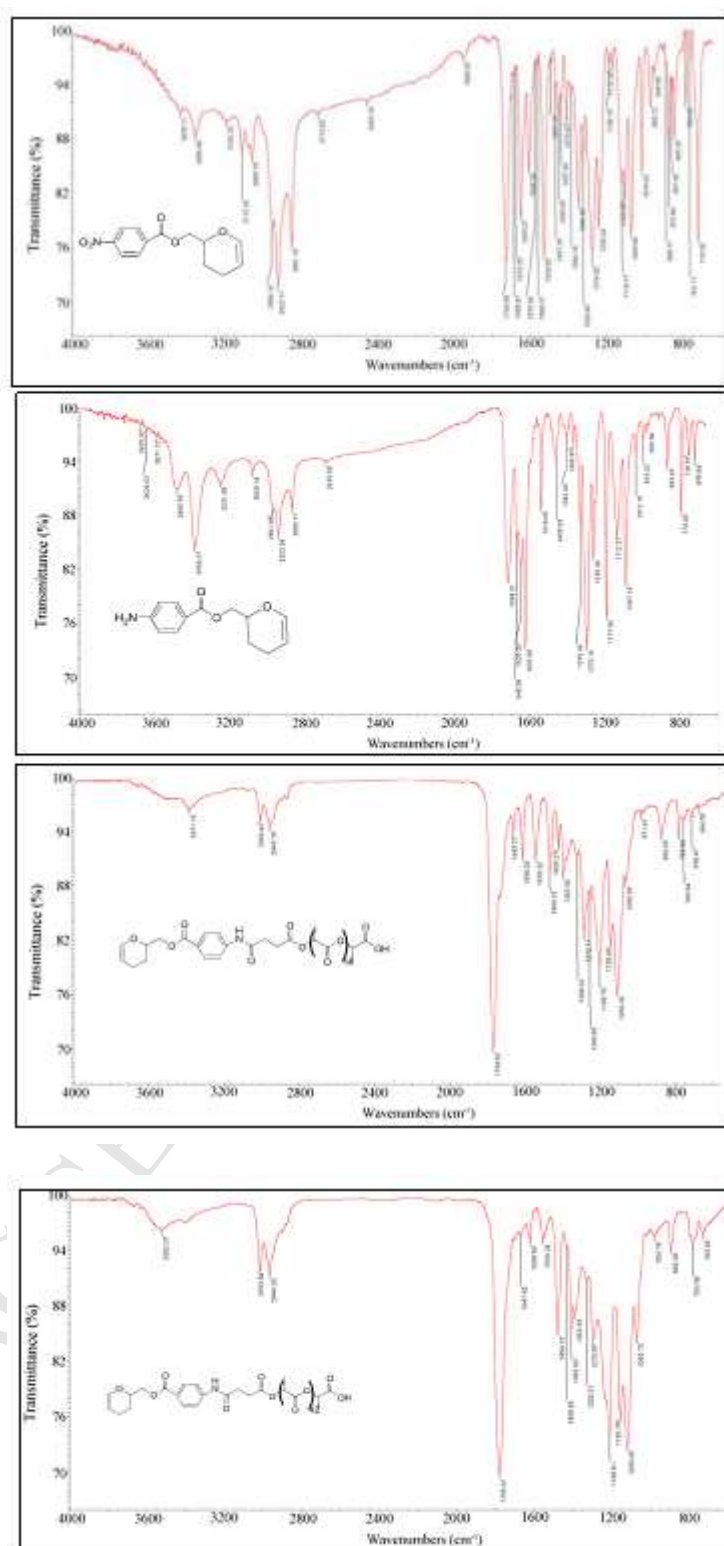
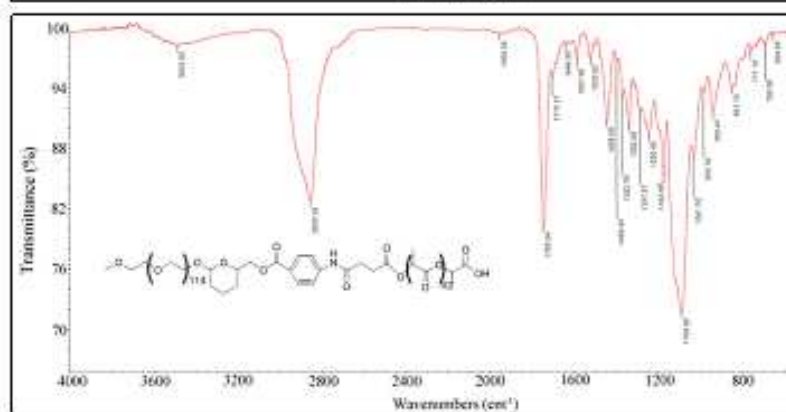
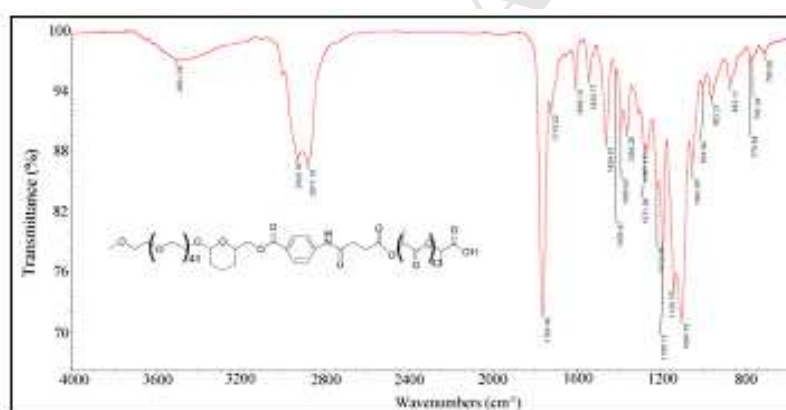
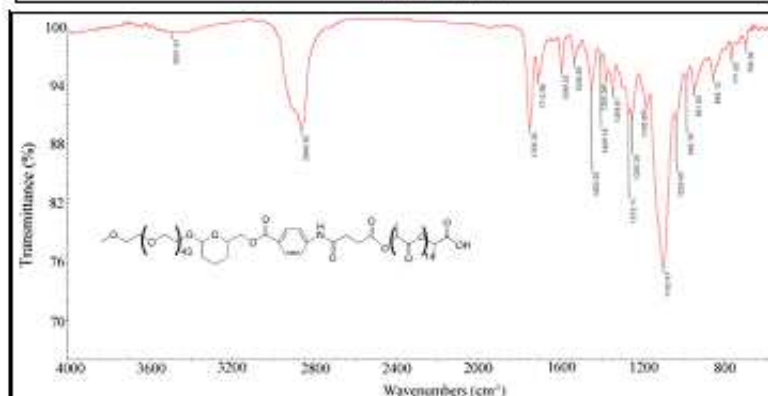
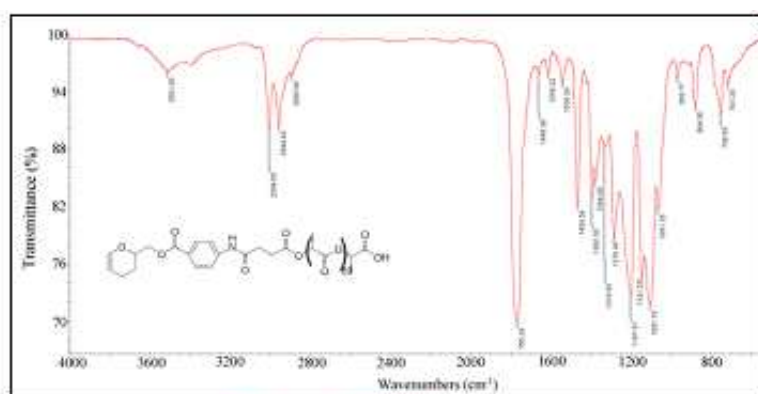
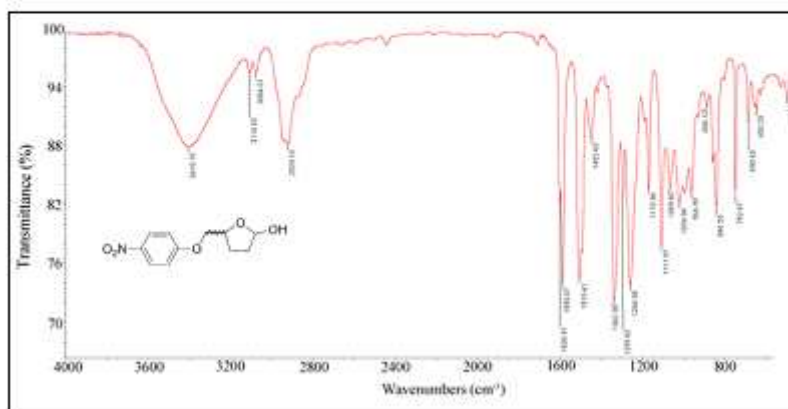
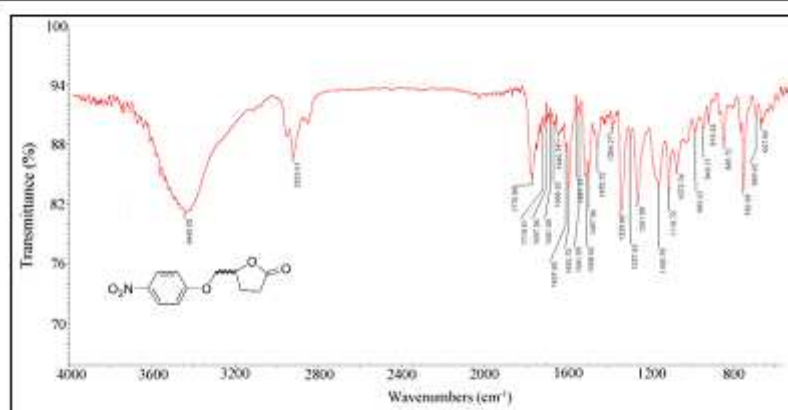
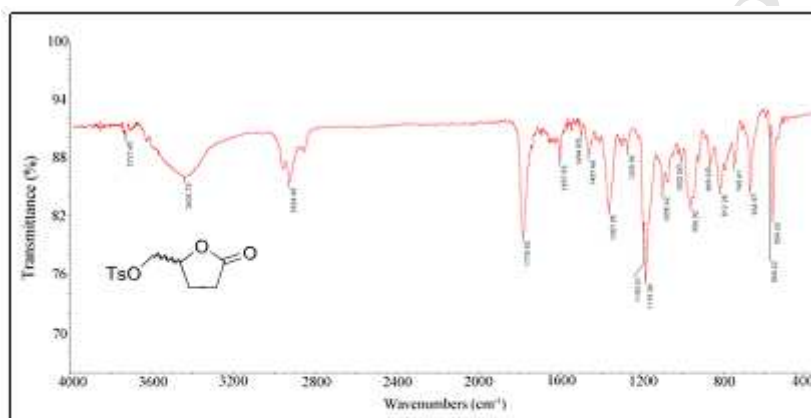
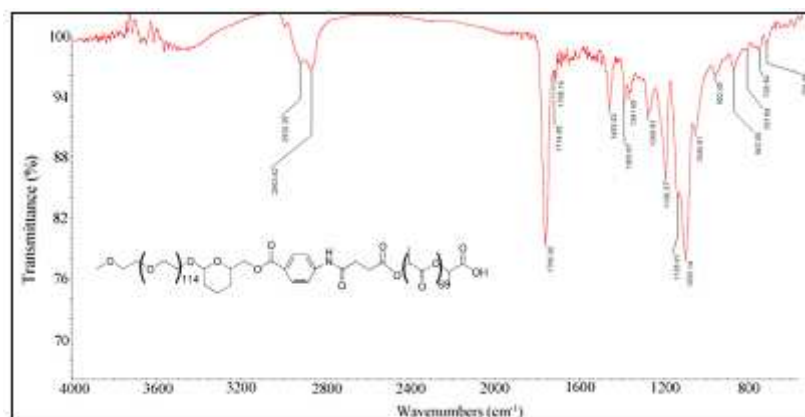


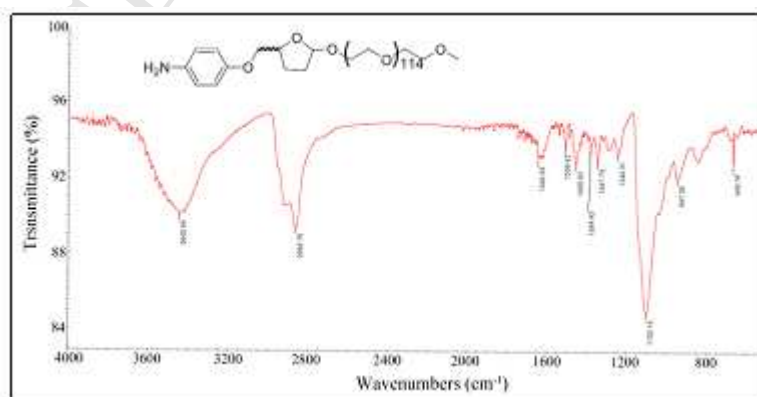
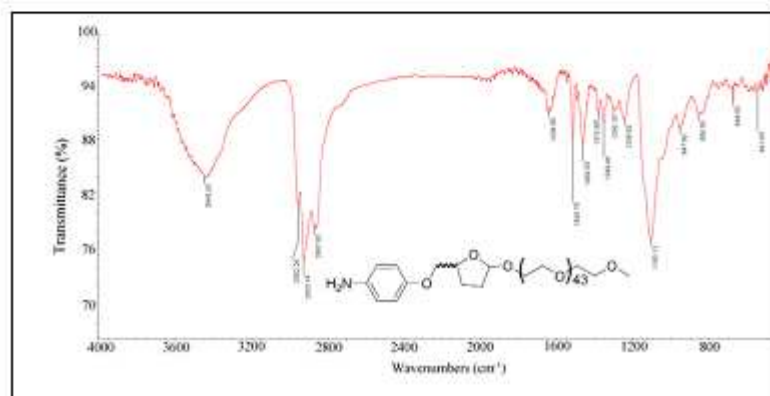
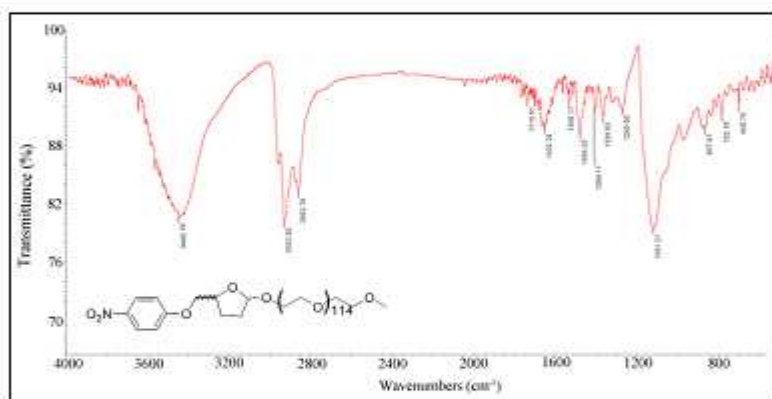
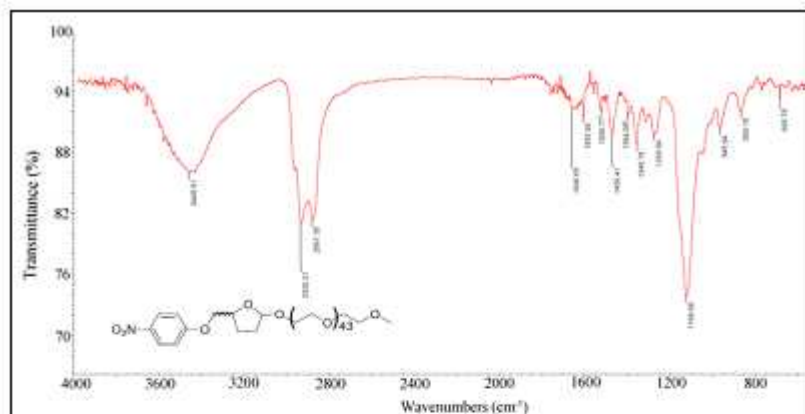
Figure S15. ^{13}C -NMR spectrum of intermediate **13** (100 MHz, CDCl_3)**Figure S16.** ^{13}C -NMR spectrum of intermediate **14** (100 MHz, CDCl_3)**Figure S17.** ^{13}C -NMR spectrum of intermediate **15** (100 MHz, CDCl_3)

3. FT-IR Spectra









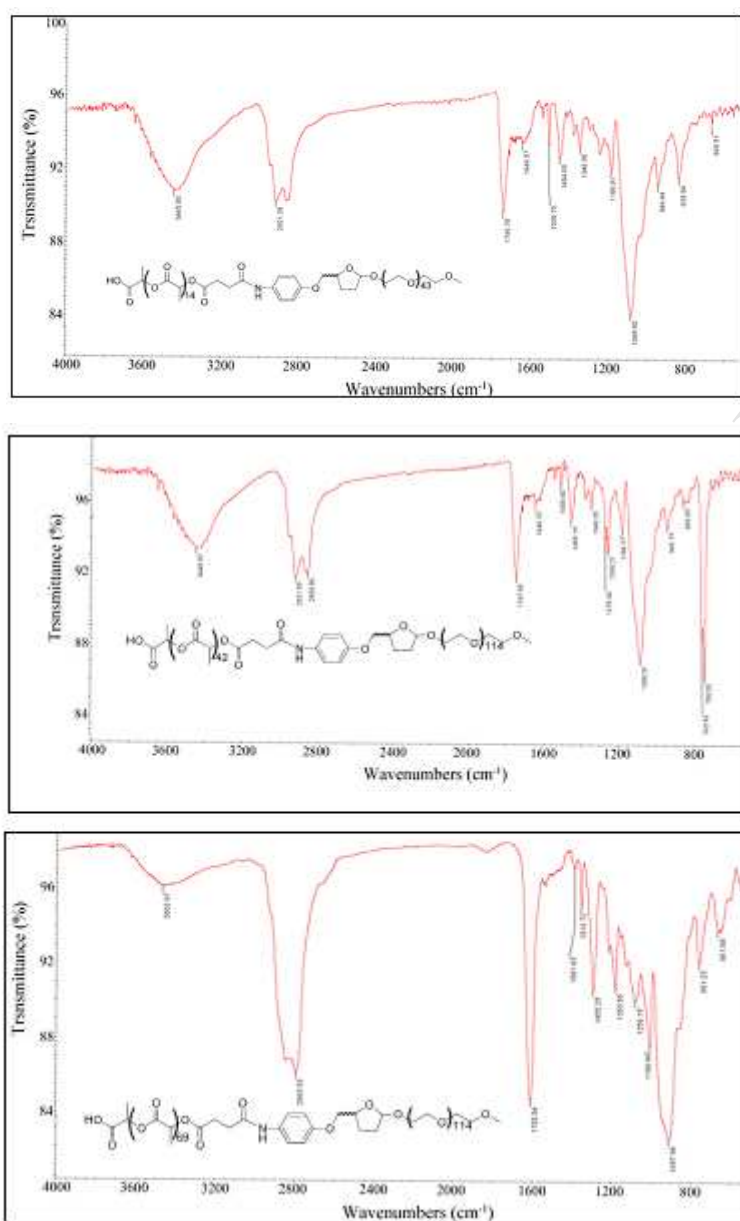
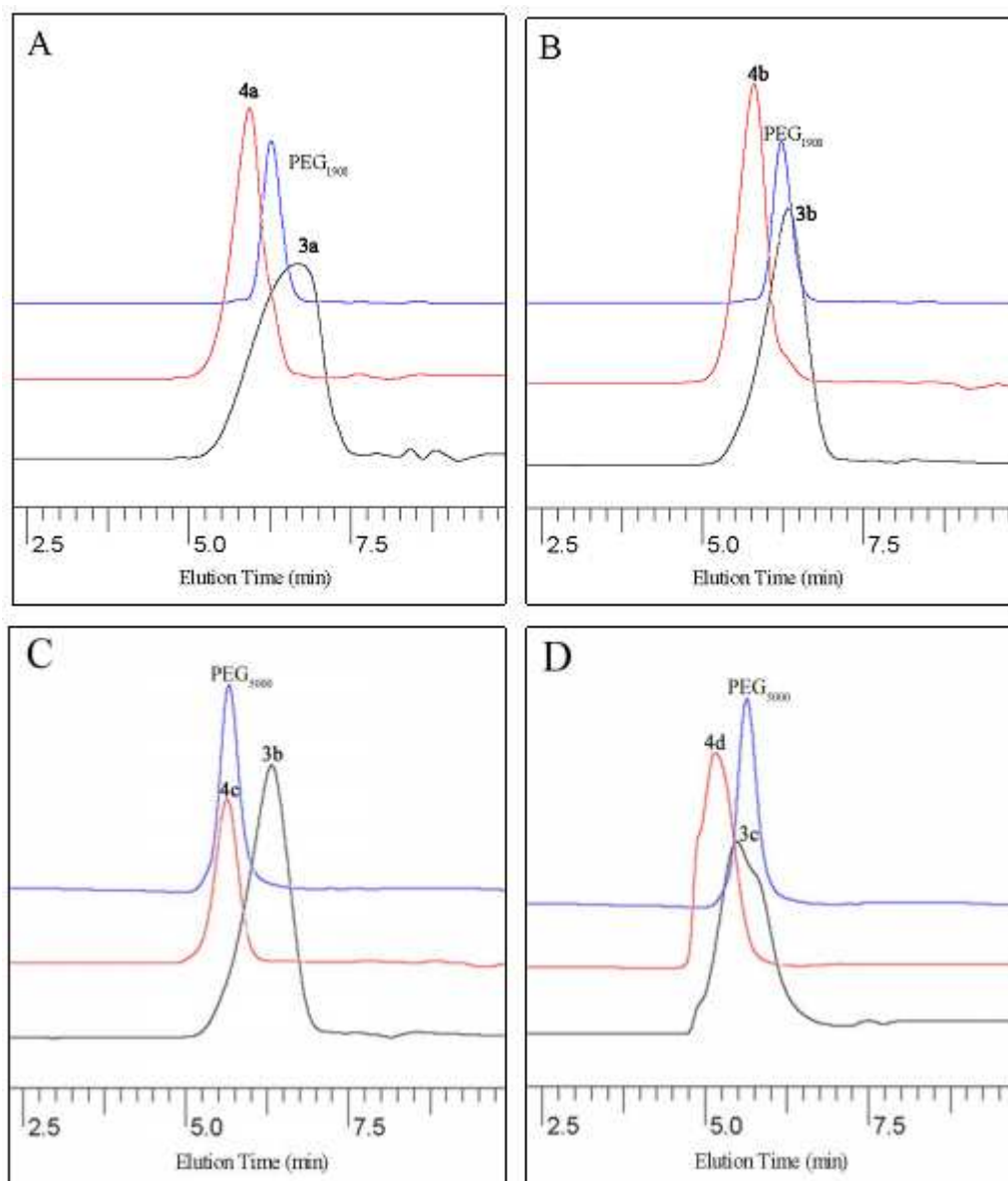


Figure S18. FTIR spectrum

4. GPC Curves of Block Copolymers



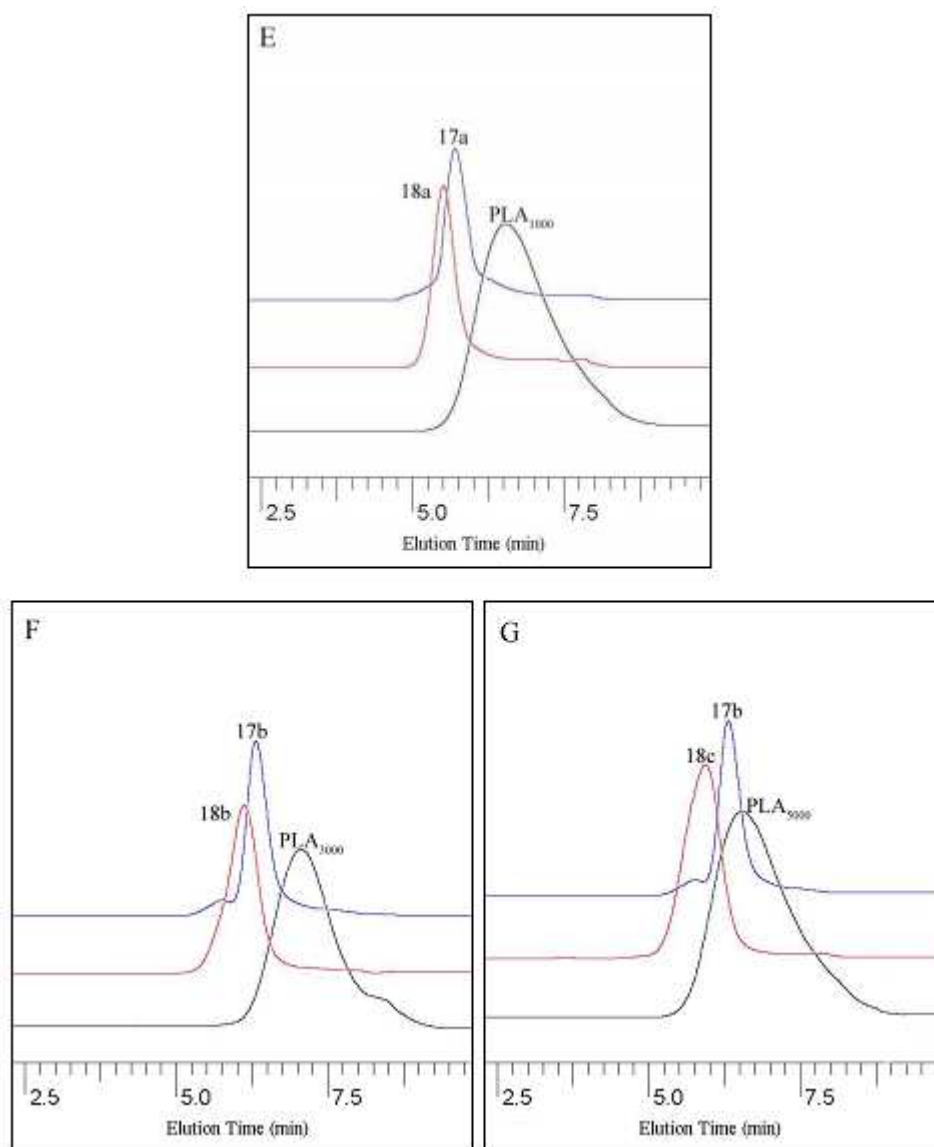
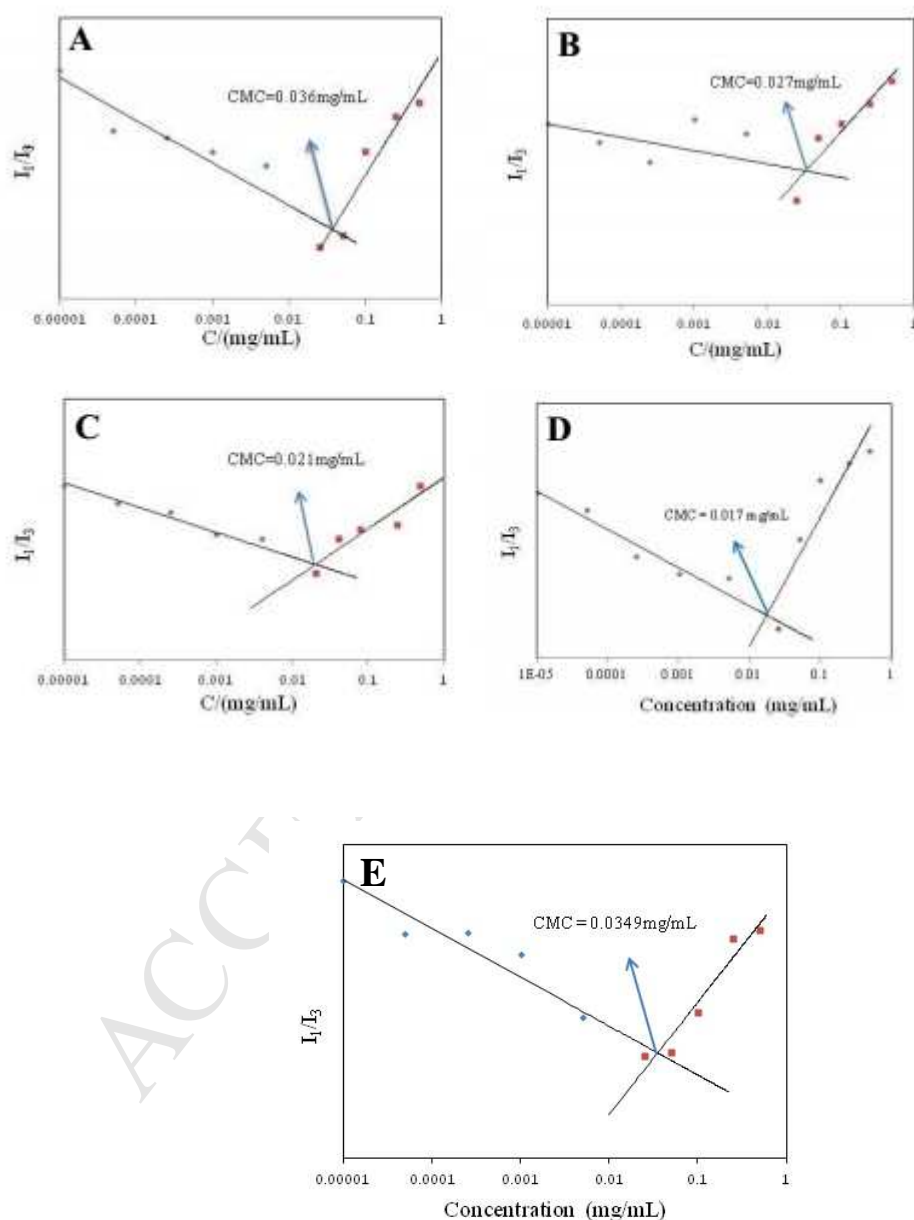


Figure S19. GPC curves of PLA-THP-PEG and PLA-THF-PEG (A) PLA₁₀₀₀-THP-PEG₁₉₀₀; (B) PLA₃₀₀₀-THP-PEG₁₉₀₀; (C) PLA₃₀₀₀-THP-PEG₅₀₀₀; (D) PLA₅₀₀₀-THP-PEG₅₀₀₀; (E) PLA₁₀₀₀-THF-PEG₁₉₀₀; (F) PLA₃₀₀₀-THF-PEG₅₀₀₀; (G) PLA₅₀₀₀-THF-PEG₅₀₀₀

5. Preparation of PLA-THP-PEG/PLA-THF-PEG Micelles

In brief, 10 mg PLA-THP-PEG and PLA-THF-PEG were dissolved in 1 mL of DMSO and stirred at room temperature for 15 min. Then, the solution was slowly added to 8 mL of deionized water and stirred for another 1 h. Subsequently, the solution was dialyzed against deionized water for 24 hrs (MWCO = 2000 g mol⁻¹), the deionized water was exchanged every 5 hrs. Water is the good solvent for linear PEG

arms and not for hyperbranched PLA core. The appearance of turbidity in the aqueous solution indicated the formation of aggregations. The critical micelle concentration (CMC) was measured by the change of fluorescence excitation spectra of pyrene in varied concentrations of block copolymers.



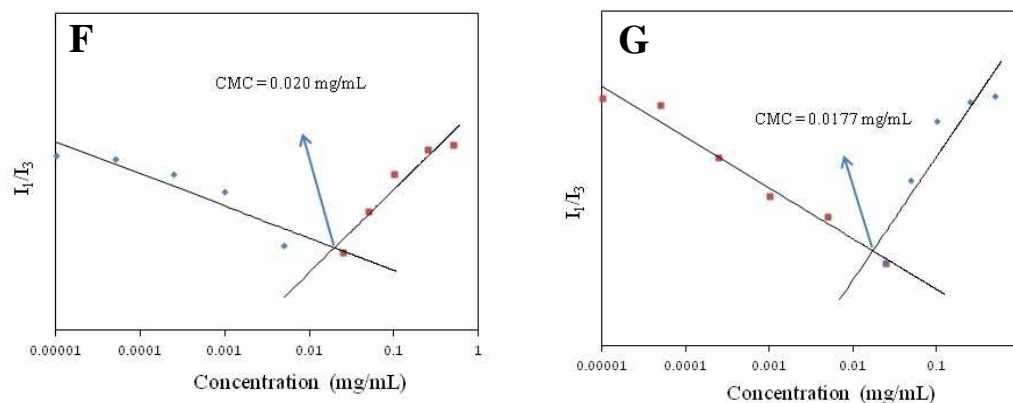


Figure S20. Relationship of the fluorescence intensity of pyrene as a function of the concentration of micelles at r.t. (A) PLA₁₀₀₀-THP-PEG₁₉₀₀; (B) PLA₃₀₀₀-THP-PEG₁₉₀₀; (C) PLA₃₀₀₀-THP-PEG₅₀₀₀; (D) PLA₅₀₀₀-THP-PEG₅₀₀₀; (E) PLA₁₀₀₀-THF-PEG₁₉₀₀; (F) PLA₃₀₀₀-THF-PEG₅₀₀₀; (G) PLA₅₀₀₀-THF-PEG₅₀₀₀

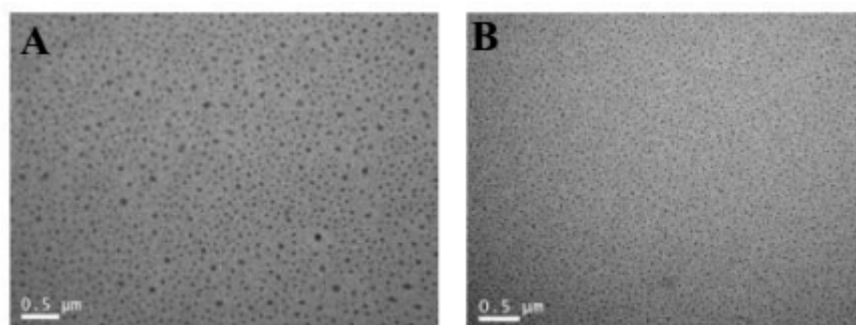


Figure S21. Representative TEM image of nanoparticles (A) PLA₃₀₀₀-THP-PEG₁₉₀₀; (B) PLA₃₀₀₀-THP-PEG₅₀₀₀ (the scale bars present 500 nm)

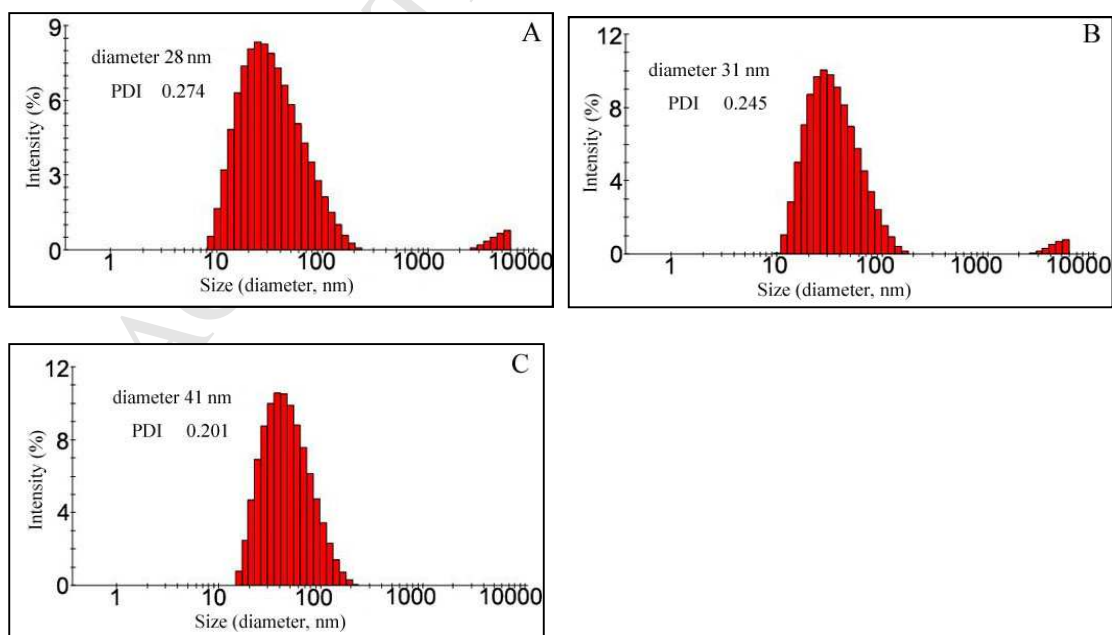


Figure S22. Representative DLS measurement of the hydrodynamic diameter of

micelles (A) PLA₁₀₀₀-THP-PEG₁₉₀₀; (B) PLA₃₀₀₀-THP-PEG₁₉₀₀; (C) PLA₃₀₀₀-THP-PEG₅₀₀₀ in aqueous solution

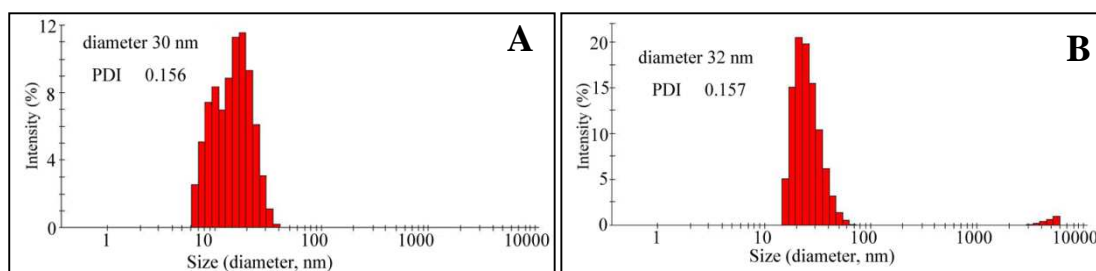


Figure S23. Representative DLS measurement of the hydrodynamic diameter of PLA-THF-PEG micelles of (A) PLA₁₀₀₀-THF-PEG₁₉₀₀; (B) PLA₃₀₀₀-THF-PEG₅₀₀₀ in aqueous solution

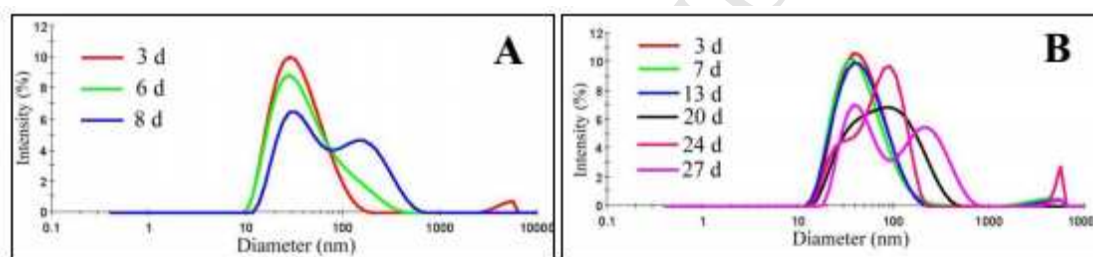


Figure S24. The stability of PLA-THF-PEG micelles (A) PLA₃₀₀₀-THF-PEG₁₉₀₀; (B) PLA₃₀₀₀-THF-PEG₅₀₀₀

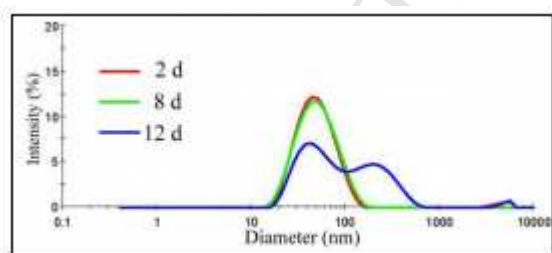


Figure S25. The stability of PLA-THF-PEG micelles PLA₃₀₀₀-THF-PEG₅₀₀₀

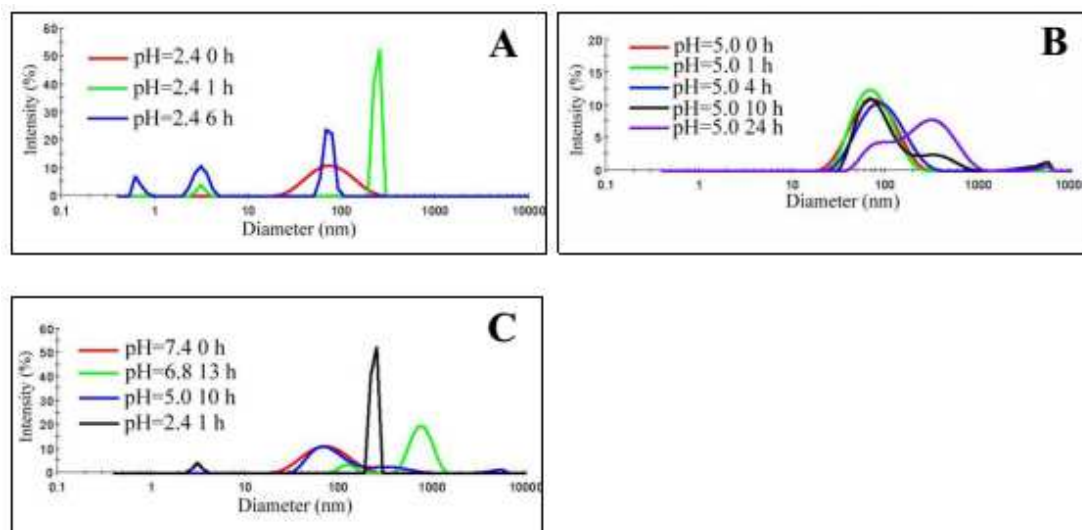


Figure S26. DLS Plots of (A) Size change of DOX-loaded PLA₅₀₀₀-THP-PEG₅₀₀₀ micelles over time (37 °C, pH = 2.4); (B) Size change of DOX-loaded PLA₅₀₀₀-THP-PEG₅₀₀₀ micelles over time (37 °C, pH = 5.0); (C) DOX-loaded PLA₅₀₀₀-THP-PEG₅₀₀₀ micelles after incubation with different pH at 37 °C.

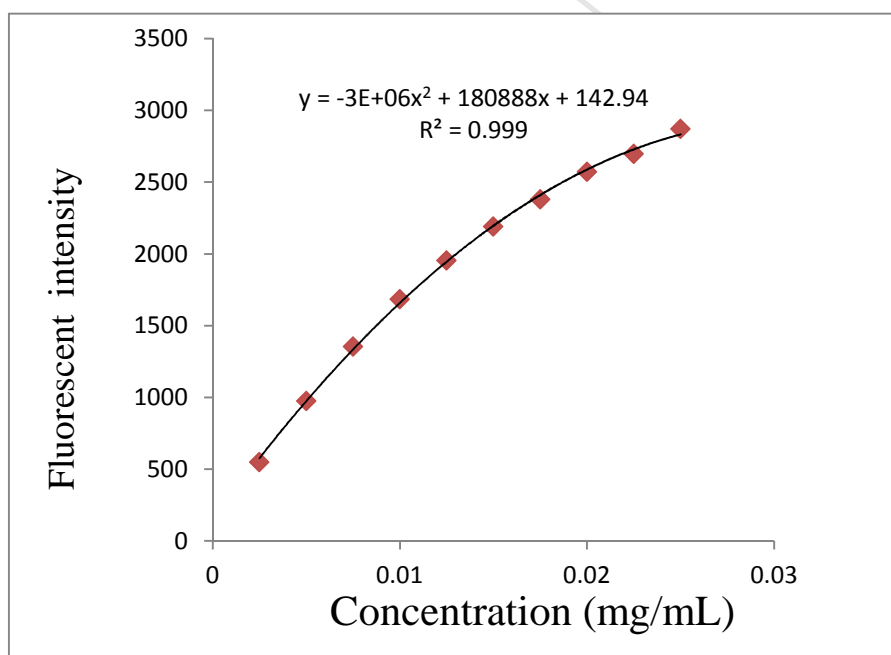


Figure S27. The calibration curve of the relationship of the fluorescent emission intensity of DOX at 485 nm and concentration in DMSO solution.